RATCHETING BEHAVIOUR OF NANO-SCALE COPPER BY CLASSICAL MOLECULAR DYNAMICS SIMULATIONS

A thesis submitted in partial fulfillment of the requirements for the degree of

Bachelor of Technology

In

Metallurgical and Materials Engineering

By

Divya (109MM0001)

Zeba Kamal (109MM0575)

Under the supervision of

Prof. Krishna Dutta

Department of Metallurgical and Materials Engineering

National Institute of Technology, Rourkela

2013

RATCHETING BEHAVIOUR OF NANO-SCALE COPPER BY CLASSICAL MOLECULAR DYNAMICS SIMULATIONS

A thesis submitted in partial fulfillment of the requirements for the degree of

Bachelor of Technology

In

Metallurgical and Materials Engineering

By

Divya (109MM0001)

Zeba Kamal (109MM0575)

Under the supervision of

Prof. Krishna Dutta

Department of Metallurgical and Materials Engineering

National Institute of Technology, Rourkela

2013

DEPARTMENT OF METALLURGICAL AND MATERIALS ENGINEERING
NATIONAL INSTITUTE OF TECHNOLOGY, ROURKELA- 769 008
ODISHA, INDIA

CERTIFICATE

This is to certify that the thesis entitled "**RATCHETING BEHAVIOUR OF NANO-SCALE COPPER BY CLASSICAL MOLECULAR DYNAMICS SIMULATIONS"**, submitted to National Institute of Technology, Rourkela by **Divya (109MM0001)** and **Zeba Kamal (109MM0575)** in partial fulfillment of the requirements for the award of the degree of **BACHELOR OF TECHNOLOGY** in **Metallurgical and Materials Engineering** is an authentic work carried out by them under my supervision and guidance. The matter embodied in the thesis has not been submitted to any other University/ Institute for the award of any degree or diploma.

Prof. Krishna Dutta
Department of Metallurgical and Materials Engineering
National Institute of Technology Rourkela

ACKNOWLEDGEMENTS

This project would not have been possible without the help, support, and cooperation of many. At the outset, we would like to express our sincere gratitude to our supervisor Prof. Krishna Dutta for his invaluable guidance and support at all times and his guidance throughout the duration of the project. We also avail this opportunity to extend our indebtedness to Prof. Natraj Yedla for his valuable guidance, constant encouragement and kind help and advice at various stages during the execution of this work. Their encouragement and comments kept our endeavors alive, and helped us to establish the overall direction of the project.

We would also like to express our gratitude to Prof. B.C.Ray, Head of the Department, Metallurgical and Materials Engineering for allowing us access to the laboratory facilities in the department.

Our sincere thanks to family and friends who have provided us with inspirational words, a welcome ear, new ideas, and their invaluable time.

Divya
Roll no: 109MM0001

Zeba Kamal
Roll no: 109MM0575

Department of Metallurgical and Materials Engineering,
National Institute Of Technology, Rourkela
Rourkela-769008

ABSTRACT

The aim of this investigation is to study the tensile and fatigue behavior of nanoscale copper at various temperatures through simulations based on molecular dynamics. The tensile stress–strain curve at various temperatures was obtained for nanoscale copper. Then, ultimate tensile strength (UTS) values of the nanoscale copper at different temperatures were determined. It was found that UTS decreases with increase in temperature. It was also observed that Young's modulus of nanoscale copper decreased with increase in temperature. Variation of tensile properties with simulation box size has also been analyzed. With increase in dimensions of the simulation box, UTS was found to decrease appreciably. The nature of accumulation of ratcheting strain varies with several parameters. Effect of few of these parameters like temperature, stress ratio, maximum stress on ratcheting behavior has been studied in this investigation. The ratcheting behavior of nanoscale copper with varying temperatures has been obtained. The accumulation of ratcheting strain was observed to increase with increase in temperature. With increase in stress ratio (R), it was observed that there is an increase in accumulation of ratcheting strain.

CONTENTS

LIST OF FIGURES

LIST OF TABLES

CHAPTER 1

INTRODUCTION

OUTLINE

Background of Research

Objectives

Summary

1.1. Background of research

Deformation under cyclic loading or fatigue is a well defined engineering problem since long. Asymmetric fatigue cycling or ratcheting is rather new domain of research where additional plastic deformation takes place during each cycle of loading; this could reduce the fatigue life of engineering components stated in the works by Xia et al. [1]. Ratcheting is a phenomenon which refers to accumulation of progressive plastic strain with increase in number of cycles; occurring under asymmetric cyclic loading [2-10]. This phenomenon is one of the low cycle fatigue responses which are currently being considered to be a critical issue for design and safety of structural components. Engineering structures which are frequently subjected to cyclic loading often undergo asymmetric stress cycling at stress states exceeding the elastic limit of the materials. Ratcheting can be considered as the average of maximum and minimum strains in a particular cycle. As ratcheting can lead to catastrophic failure of the structures, accurate prediction of ratcheting response is essential.

Rider et al. [2] have reported that ratcheting deformation generally occurs in the direction of mean stress; for ductile materials ratcheting extension is necessarily accompanied by a ratcheting contraction in orthogonal directions. It can also be stated that fatigue performance of materials under a range of temperatures may vary. Investigations regarding the influence of temperature on low-cycle fatigue behavior of nickel-based superalloys have been made by Chen et al. [14]; it was found out that with increase in temperature, fatigue life did not monotonously decrease. However, conducting fatigue experiments at high temperature is really a challenge and needs prolonged duration of time. Hence many simulation studies have come into picture to predict the fatigue behavior of materials at varying temperatures.

Using molecular dynamics (MD) simulation, fracture mechanisms of nanoscale pure iron under static and symmetric cyclic loading conditions have been performed by Inoue et al. [15]. Li and his co-workers [16] investigated the cyclic stress/strain evolutions for multi-axial fatigue-life prediction through simulation studies; it was found that the improvement of fatigue life prediction depends not only on the fatigue damage models, but also on the accurate evaluations of the cyclic elasto-plastic stress/strain responses. The tensile and fatigue behavior of nanoscale copper with vacancies at various temperatures has been studied using MD simulation by Chang [17]. Chang and Fang investigated the influence of tensile and fatigue behavior of nanoscale copper through MD simulation [18]. However all the existing research works, as per the knowledge of the current authors, are based on application of symmetric cyclic loading to understand the low cycle or high cycle fatigue behavior of nanoscale materials. Whereas, studies related to ratcheting deformation of nanoscale copper using MD simulation is lacking. The mechanical properties of nano-structured copper have been of significant interest to researchers since the development of electronic industry. Earlier investigators have studied the properties of nanoscale copper under static loading while very few studies have been conducted to test the effect of cyclic loading as it consumes a lot of time when the experiment is conducted in real life.

In this investigation, the tensile behavior of nanoscale copper has been examined over a range of temperatures. In association to that, asymmetric fatigue cycling or ratcheting experiments have been carried out up to a specified number of cycles to understand the nature of strain accumulation in nanoscale copper. These are done at different temperatures and stress ratios. Finally, a comparative study has been made between the ratcheting behavior assessed using MD simulation and earlier experimental reports conducted under similar loading conditions.

1.2. Objectives

The main objectives and the relevant work-plan to fulfil these can be broadly summarized as:

(I) To find tensile behaviour of nanoscale copper at various temperatures:

This part consists of (a) generating plots for tensile stress vs. strain curves of nanoscale copper at different temperatures, (b) calculating the ultimate tensile strength of nanoscale copper at different temperatures, (c) determination of Young's Modulus at various temperatures and (d) observing variations in ultimate tensile strength with box dimensions.

(II) To study the nature of strain accumulation due to ratcheting in nanoscale copper:

To fulfil this objective experiments are conducted on (a) investigations related on variations in accumulation of ratcheting strain with number of cycles for different stress ratios (b) investigations on ratcheting strain with number of cycles at (i) varying maximum applied stress and constant stress ratios (ii) fixed maximum applied stress and constant stress ratios at different temperatures.

(III) To compare observed simulations results with those in previous studies on ratcheting behaviour of nanoscale copper:

A comparison of the nature of ratcheting strain has been made with those in the previous studies of nanoscale copper. The results obtained from simulations in this investigation have been compared with those obtained in previous studies conducted through laboratory experiments to understand ratcheting behaviour of bulk materials.

1.3. Summary

The thesis has been ordered into five chapters. There is briefing of the significance of the problem and the motivation behind this investigation in **Chapter-1**. Some relevant literature background related to the current investigation of fatigue loading and molecular dynamics simulation has been presented in **Chapter-2**. **Chapter-3** consists of simulation parameters to perform simulation studies on nanoscale copper along with the description of the program codes behind these simulations. **Chapter-4** includes the results and discussion corresponding to the above stated objectives. **Chapter-5** is an overview of the conclusions derived from this investigation which has been summarized together briefly with few directions for future work related to this area. A comparison has also been made with the results obtained from this investigation with those of previous studies. All references cited throughout the work have been compiled at the end of **Chapter-5**.

CHAPTER 2

Literature Survey

OUTLINE

Introduction

Fatigue: Some basics

Cyclic loading behaviour of materials

Ratcheting phenomenon

Factors affecting accumulation of ratcheting strain

- **Effect of mean stress**
- **Effect of maximum stress**
- **Effect of stress ratio**
- **Effect of temperature**
- **Material dependence**

Molecular dynamics simulation

Advantages of using molecular dynamics simulation

Review of the current problem

2.1 Introduction

In this present work, the ratcheting fatigue behaviour of nanoscale copper is dealt with. It is known that under conditions of asymmetric cyclic loading accumulation of ratcheting strain occurs. There have been extensive reports on fatigue behaviour of materials under symmetric loading over the last century. Fatigue behaviour of materials under symmetric loading is governed by their microstructure, chemistry, strength, ductility, surface condition and residual stress [25, 26]. There is availability of large volume of literature that has effects of the parameters which are mentioned above. However, there are limited reports on ratcheting behaviour of materials which are correlated to the effect of these factors. It is thus required to have a brief knowledge about the works till date that are done on the ratcheting behaviour of materials. In order to have further understanding in this context, acquaintance with the current level of information and works till date on ratcheting behaviour has to be made.

There is very limited knowledge on ratcheting behaviour of materials. It has thus induced great interests in investigators for further research in this field in the last two decades. In the different sections of this chapter, there has been an overview of the works that has been done on ratcheting behaviour of materials. In the beginning, there has been a discussion on the general aspects of cyclic loading in section 2.2 followed by material response during cyclic loading in section 2.3. The phenomenon of ratcheting and its significance are discussed in section 2.4. A brief compilation has been made in section 2.5 about the literature which shows the affect of different experimental and material parameters on accumulation of ratcheting strain. There has been a brief introduction about molecular dynamics simulation in the section 2.6. This has been followed by stating the advantages of using molecular dynamics simulation in section 2.7.

Conclusion of this chapter has been made by stating an appraisal on the current problem in section 2.8.

2.2 Fatigue: Some basics

A well accepted fact that today due to fatigue there is occurrence of almost 90 percent of all service failures [25]. Structural components usually are seen to fail at stress levels appreciably lower than their monotonic fracture strength values, which are being subject to repeated cyclic loading and unloading over a long period of time. This is commonly termed as fatigue failure [25,26]. However, nature of the type of cycles during loading may vary. Categorization of fatigue into two broad regimes, namely high cycle fatigue (HCF) and low cycle fatigue (LCF), is be done depending upon the number of cycles (N) that a material is able to withstand before failure occurs. When $N \geq 10^5$ cycles, type of failure can be categorized as HCF and when $N < 10^4$ or 10^5, it is called LCF.

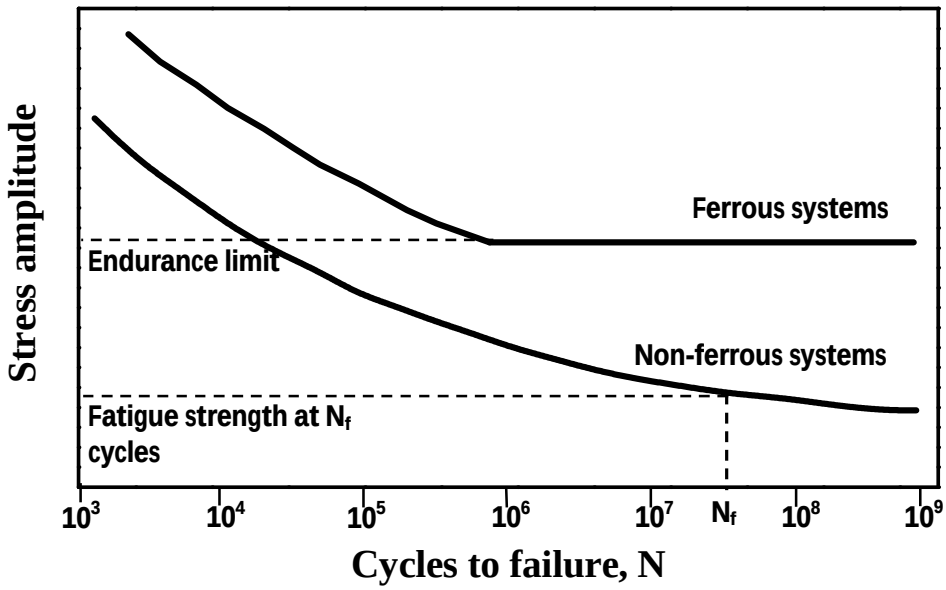

Fig. 2.1: Schematic representation of the *S*-*N* curve.

Historically, there has been immense focus on those situations in which there is requirement of more than 10^5 cycles to failure with low stress value (i.e. generally 30% of yield stress) and the nature of deformation is mainly elastic. In high-cycle fatigue situations, to characterize materials' performance a plot indicating the magnitude of cyclic stress (*S*) against cycles to failure (*N*) in logarithmic scale referred to as *S-N* curve is shown in Fig. 2.1

There is existence of a particular level of stress below which a material is able to withstand infinite number of cycles without occurrence of failure. This stress level is referred as fatigue limit or endurance limit. Under this category lie several ferrous systems. To the contrary, non-ferrous systems, particularly aluminum and aluminum-based alloys do not possess any well-defined level of stress below which there is no failure of these materials and therefore, for non-ferrous systems, it is very crucial to define the endurance limit. Basquin equation is used to define the *S-N* curve in HCF:

$$N\sigma_a^p = C \qquad \textbf{(2.1)}$$

where: σ_a = stress amplitude;

N = number of cycles;

p and *C* are empirical constants.

When a state comes where stress is high enough for plastic deformation to occur, then it is noticed that description of fatigue behaviour in terms of stress is of less help while strain in the material results in a simpler description. According to Coffin-Manson relation, LCF test results can be represented in a usual way by plot of plastic strain range versus *N*:

$$\frac{\Delta\varepsilon_p}{2} = \varepsilon_f'(2N)^{C_1} \qquad \textbf{(2.2)}$$

where: $\Delta\varepsilon_p/2$ is the plastic strain amplitude;

ε_f' is an empirical constant known as the fatigue ductility coefficient, the failure strain for a single reversal;

$2N$ is the number of reversals to failure (N cycles);

C_1 is an empirical constant known as the fatigue ductility exponent, commonly ranging from -0.5 to -0.7 for metals.

A typical log-log plot of $\Delta\varepsilon_p$ *vs.* N is shown in Fig. 2.2. Consideration of low cycle fatigue is generally done during design of steam turbines, nuclear pressure vessels and other type of power machineries, structures where seismic loadings are executed and so on. It has been a usual practice of doing tests related to LCF at frequency less than 1 Hz.

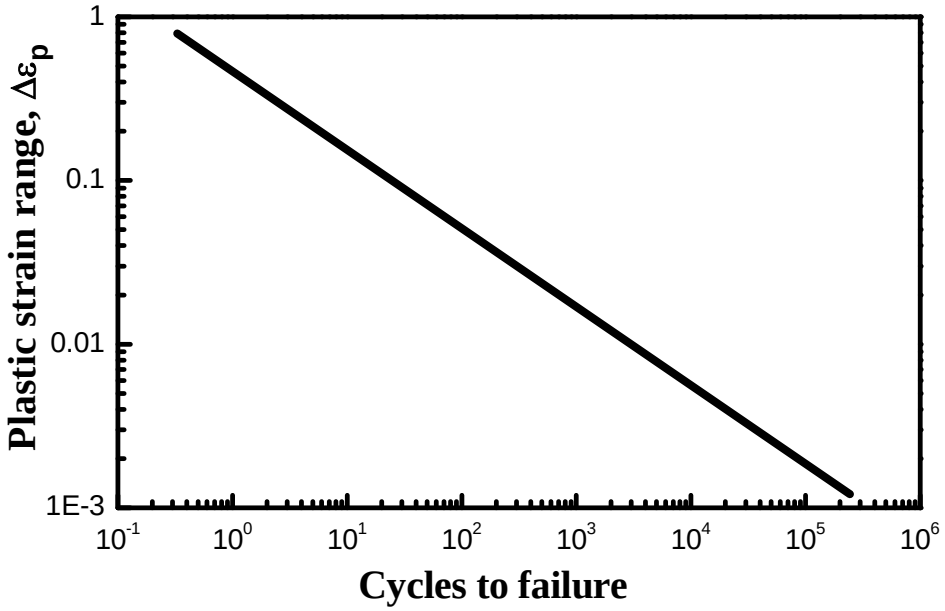

Fig. 2.2: Low cycle fatigue curve ($\Delta\varepsilon_p$ vs. N) [25].

Although fatigue is conventionally considered to be of two types, viz. LCF and HCF, but recent studies also shows the existence of very low cycle fatigue (VLCF) [5] and very high cycle fatigue (VHCF) [3].

Failures which occur in less than 100 cycles can be described as very low cycle fatigue [5]. There have been reports by Xue which suggests that Coffin-Manson equation does not fit well in the category of VLCF. Hence, life prediction and the reported failure mode of a material in this category should be different. On the other hand, it is reported that components which fall under VHCF category fails at $N_f > 10^7$.

In general, the fatigue life of a material depends on the parameters like: microstructure of the material, type of processing, geometry of the component, nature of loading and environment in which application takes place.

The history of the growth of fatigue cracks can suitably be sub-divided into three stages:

(i) Crack Initiation, (ii) Incremental Crack Growth, and (iii) Final Fracture.

For the reason that there is existence of higher stresses and a very high probability of the presence of defects (existence of corrosion pits, scratches, eroded or corroded areas, etc.) at free surfaces, fatigue crack initiation usually occurs at these locations. Through repeated micro-plastic deformation, even at highly-polished defect-free surfaces, there can be initiation of fatigue cracks that result in the formation of the so called “intrusions” and “extrusions” on the surface. The intrusions, which subsequently lead to the formation of micro-cracks, actually can act as sites for local stress concentration. The crack, in a crystallographic fashion, grows at a slant in Stage I. On dominance of a striation forming mechanism, cracks gradually deflect into a Stage II crack. Through repeated crack tip blunting and sharpening effects, fatigue crack

propagation occurs; which is actually due to micro-plastic deformation mechanisms which are being operated at the crack tip. There can be occurrence of crack propagation over a long period of time;characteristic markings which are called “beach markings” or “clam shell markings” may be contained by the fracture surface. These occurrences of different *periods* of crack growth can be reflected by the markings which are recognizable and can be seen even by naked eye. At intervals of the order of 0.1 μm or more, extremely fine parallel markings can be observed which are called as “striations”, which can be seen using electron microscopes under high magnifications and theserepresent the crack growth due to *individual* loading cycles. There are two primary mechanisms via which striations arise: alternating slip and crack tip blunting and re-sharpening. A sketch below in Fig 2.3 can be used to represent these mechanisms.

Limited crack tip plasticity results in occurrence of alternating slip, as a result of which there is movement of dislocations only on a few parallel planes. Due to application of load at the crack tip, the dislocations are produced which have a tendency of piling up close to the crack tip; these pile up of dislocations results in localized work hardening. As a result of this work hardening there is large possibility of embrittlement of the material, thus making the growth of the crack easier on the slip plane. With the growth of crack, activation of new slip planes occur, and repetition of the process takes place as illustrated above. With the alteration of the slip planes a “zig-zag” path is followed by the crack and on the failure surface there is formation of sharp ridges. In materials which are capable of more generalized yielding at the crack tip, crack tip blunting and re-sharpening occurs. Due to plastic deformation occurring under application of load, blunting of the initially sharp crack happens. A small extension is caused by this blunting action in the crack length. On unloading of the crack, due to the presence of an elastic stress field

around the plastically relaxed crack tip the crack tends to re-sharpen. With repetition in loading of the crack, blunting occurs again, thus a ripple on the surface is left behind.

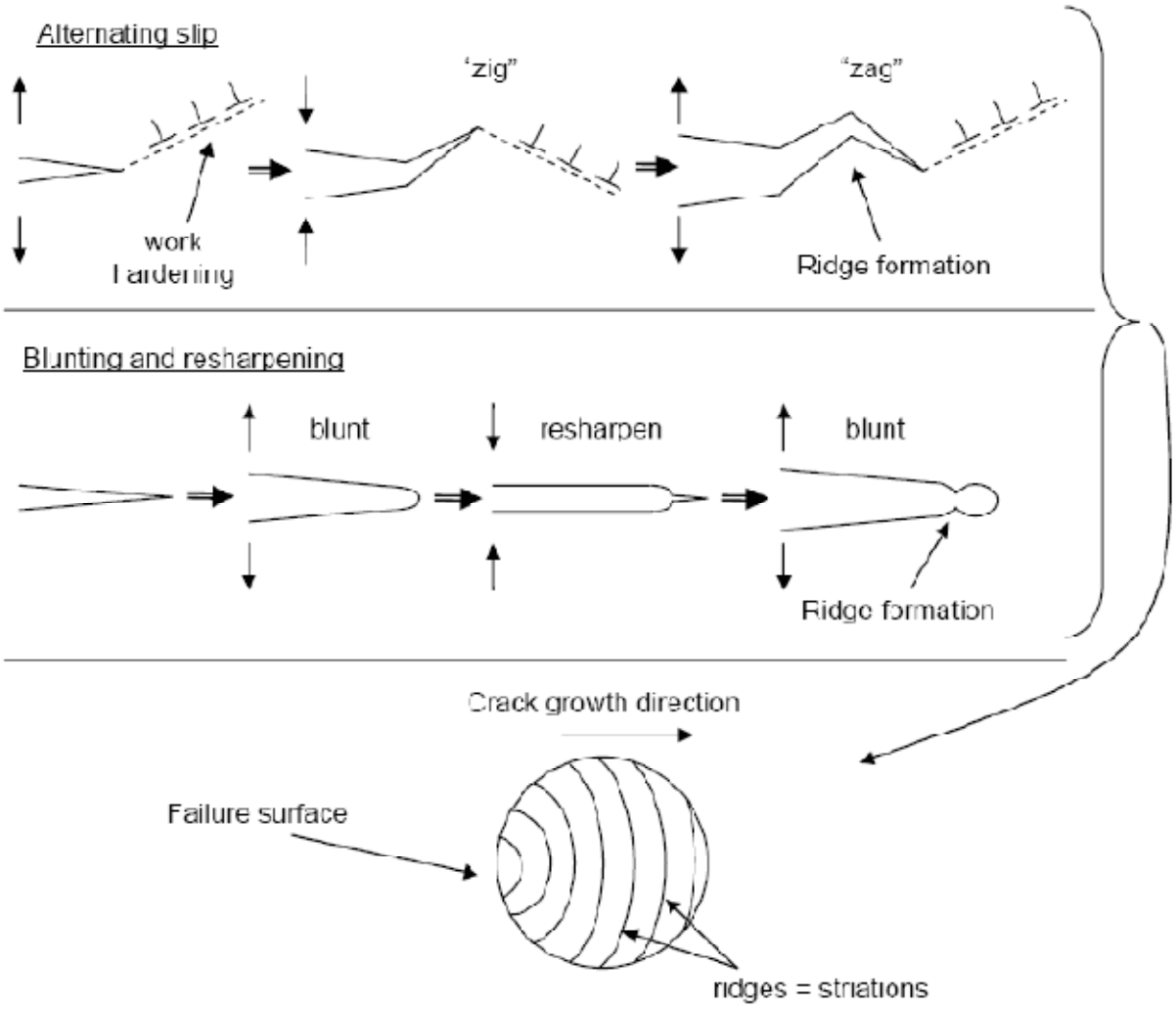

Fig. 2.3: Schematic representation of mechanisms of fatigue crack growth.

Further on, in Stage III, there occurs the superimposition of static fracture modes on the growth mechanism, till finally catastrophic failure occurs by shear at an angle to the direction of growth. A schematic representation illustrating the various stages of fatigue crack growth isshown in Fig 2.4.

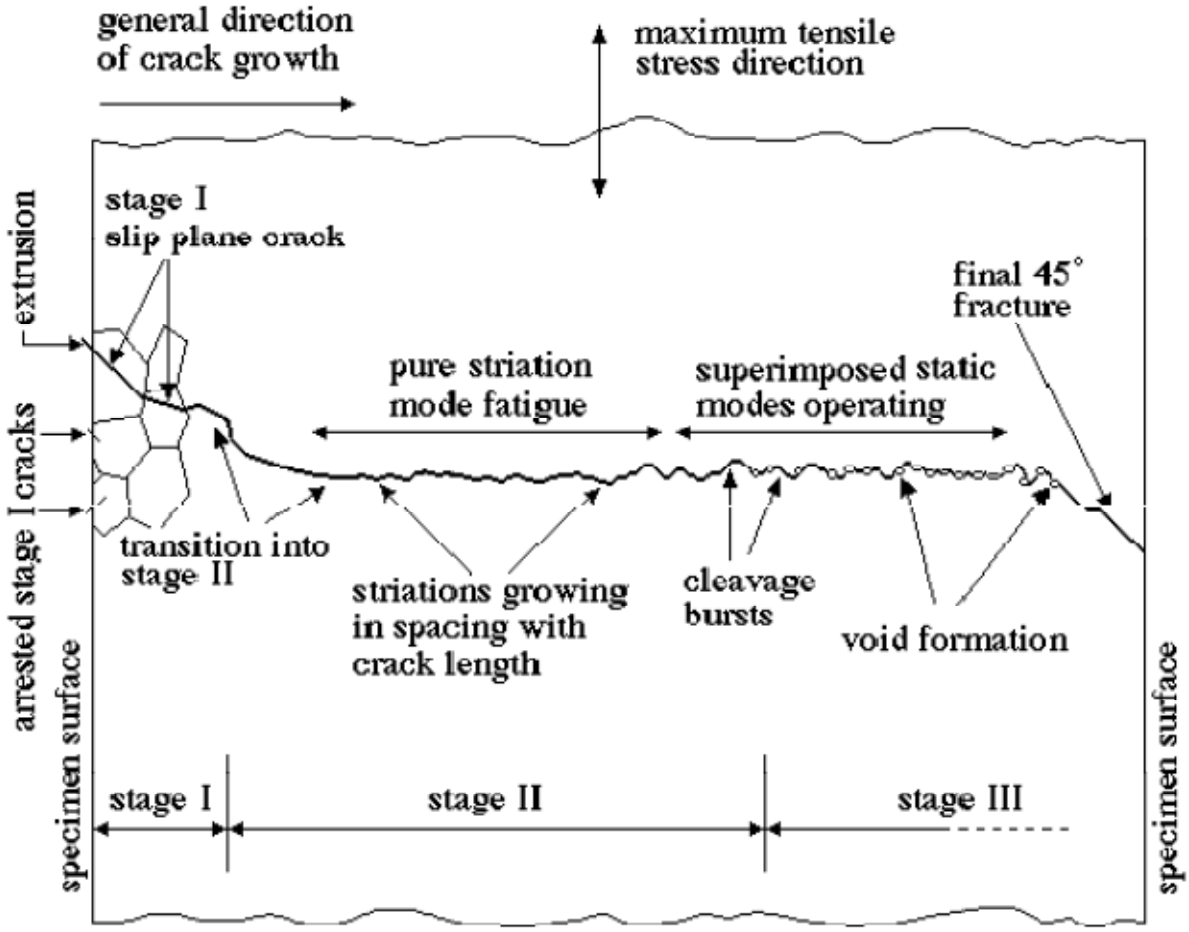

Fig. 2.4: Schematic representation of the various stages of fatigue crack growth.

2.3 Cyclic loading behaviour of materials

Depending upon the mode of input control variable, whena specimen is subjected to cyclic loading, response of the material to the cyclic deformation differs as illustrated schematically in Fig. 2.5 [4]. Throughthis type of experiments, characteristics of different materials can be illustrated easily. The response can be cyclic hardening or cyclic softening if the control variable is strain (details in section 2.5). In the presence of a mean strain, mean stress relaxation may occur. Similar to the strain-controlled tests, the material may show strain

hardening or strain softening for case of fully reversed stress-controlled loading (further details in section 2.5).The rate at which plastic strain accumulation takes place decreases with the number of cycles and finally reaches to a stable state for cyclically hardenable materials while for cyclically softenable materials, the reverse phenomenon occurs.

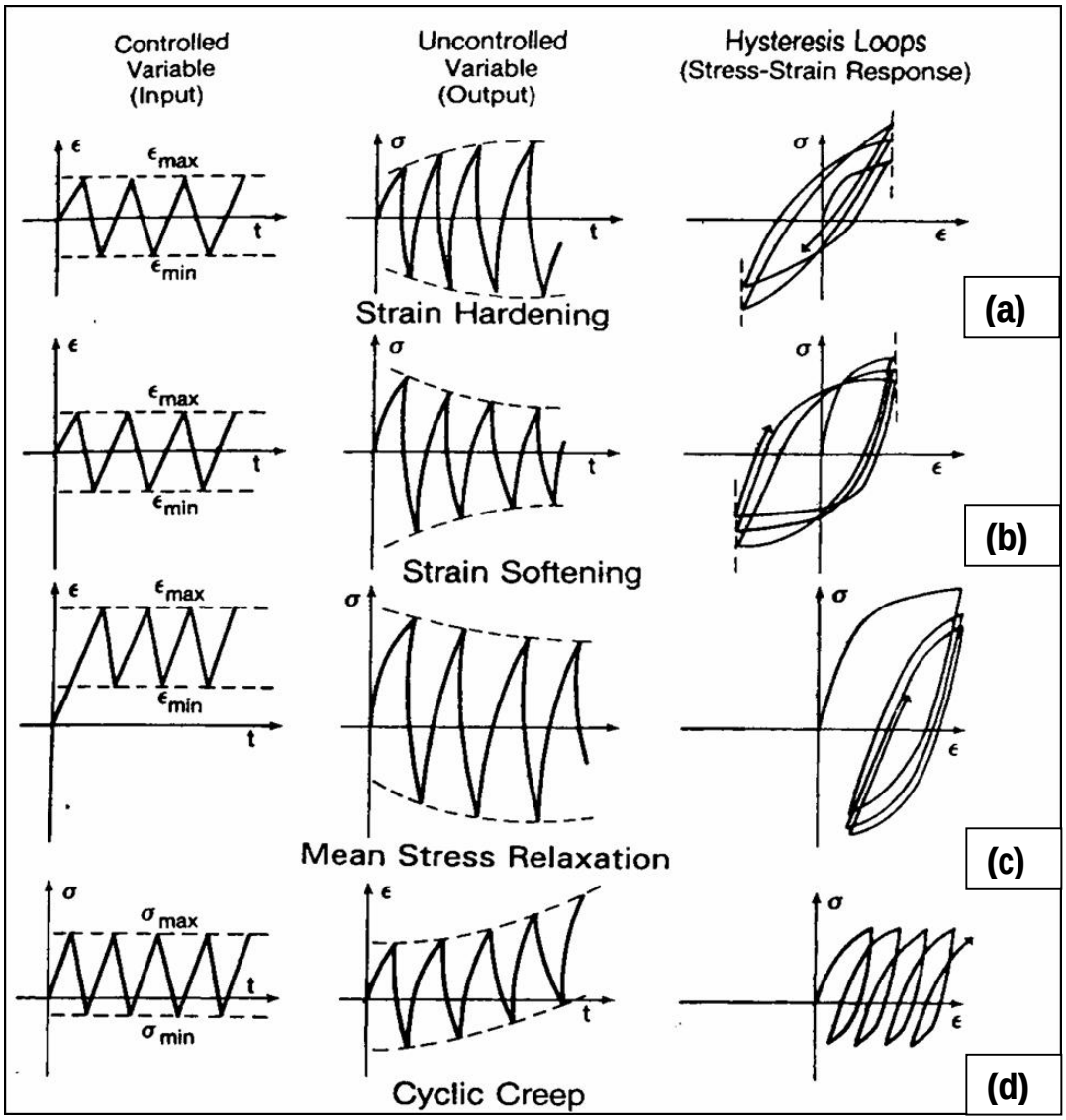

Fig. 2.5: Schematic material response to various modes of cyclic input variables: (a) row 1- control: mean strain = 0, material response: strain hardening, (b) row 2- control: mean strain = 0, material response: strain softening, (c) row 3- control: mean strain > 0, material response: mean stress relaxation, (d) row 4- control: stress (mean stress ≠ 0), material response: cyclic creep or ratcheting(following [4]).

The material response is not clearly stated till date in the case of asymmetric loading; difference in responses has been observed when the control variable is stress. Due to the presence of non-zero mean stress, there will be additional accumulation of strain, in each cycle of loading. In the present work, it is referred as 'ratcheting'.

2.4 Ratcheting phenomenon

Ratcheting as discussed in the previous section occurs when asymmetrical cyclic loading is applied to structural components. There is formation of hysteresis loops in each cycle of loading which can be seen in Fig. 2.5; it illustrates that there is variation in nature of these loops with increasing number of cycles. There is translation of the hysteresis loops towards the direction of higher plastic strain; this occurs due to the nature of ratcheting deformation produced for subsequent cycles. The phenomenon is schematically illustrated in Fig. 2.5(d) and detailed clarification of the phenomenon has been shown in Fig. 2.6. As stated by Ringsberg [6] in his works there are instances where for every cycle of loading, the material shows additional plastic deformation known as ratcheting. Until the exhaustion of material ductility takes place till then there is continuation of accumulation of deformation and finally the material ruptures; although it is obvious that the rate of strain accumulation continuously decreases with increasing number of cycles, which further indicates material response towards a steady state. Numerically, ratcheting strain is measured as the mean strain for a particular cycle [12, 13] and it is expressed as:

$$\varepsilon_r = (\varepsilon_{max} + \varepsilon_{min})/2 \qquad \textbf{(2.3)}$$

where: ε_r is ratcheting strain;

$\varepsilon_{max}$is the maximum strain at a particular cycle;

$\varepsilon_{min}$is the minimum strain at the cycle.

A different definition of ratcheting is also found in the literature. Lim et al. [20] have used the expression of ratcheting strain as:

$$\varepsilon_r = (\varepsilon_{max} + \varepsilon_{min})/2 - (\sigma_m/E) \quad \textbf{(2.4)}$$

where:

σ_m is mean stress;

E is elastic modulus of the material.

The parameters which are used to define ratcheting strain by equations 2.3 and 2.4 (i.e. ε_r, ε_{max}, ε_{min}, σ_m) are shown in Fig. 2.6. The expression of ratcheting strain suggested by Lim et al. [20] is yet to gain popularity which considers only the plastic component of ratcheting strain.

2.5 Factors affecting accumulation of ratcheting strain

There are different parameters that affect strain accumulation by ratcheting. As illustrated in Fig. 2.7, these may be mostly classified as: **type of loading, working temperature of the material** and **characteristics of the material undergoing investigation**. The types of loading indicate how there is imposition of cyclic loading on the material, and these are specified in terms of **mean stress, stress amplitude maximum stress, stress rate and stress ratio**. Apart from **working temperature**, there is dependence on the various material parameters like the **chemistry of the material,** and its **cyclic hardenability** or **cyclic softenability.**

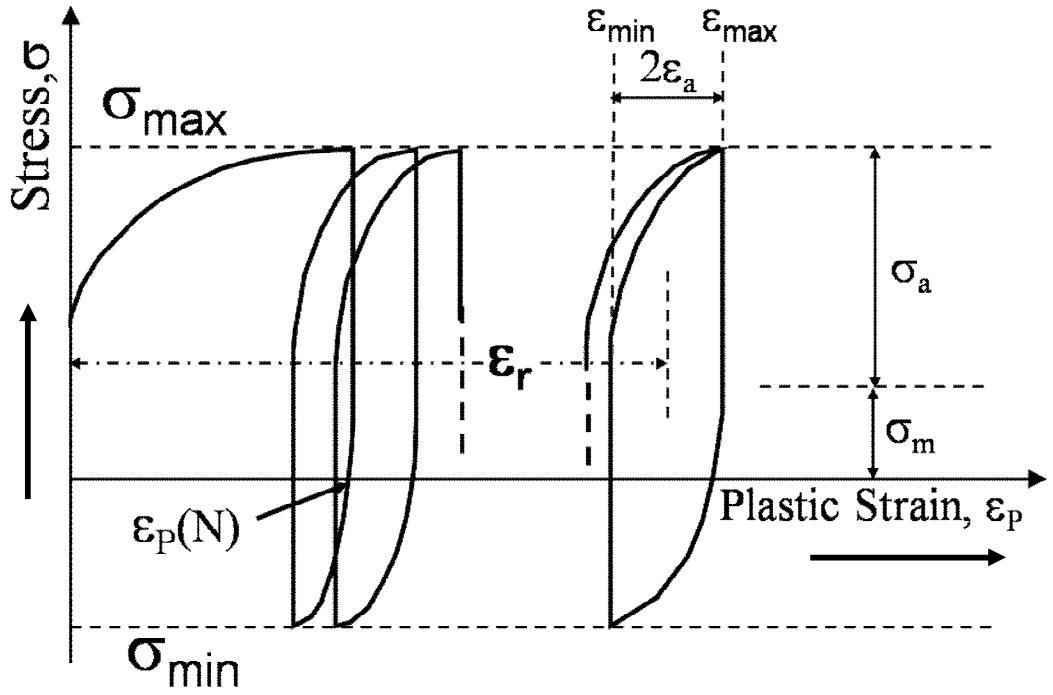

where:

σ_{max}= Maximum stress; σ_{min} = Minimum stress;

σ_m= Mean stress; σ_a = Stress amplitude;

ε_P =Plastic strain; ε_a = Strain amplitude;

ε_r = Ratcheting strain

Fig. 2.6: Schematic illustration of ratcheting procedure.

2.5.1 Effect of mean stress

The most important factor that affects strain accumulation during ratcheting is usually mean stress (σ_m). It is reported that strain accumulation during ratcheting occurs due to presence of positive or negative mean stress as investigated by many groups [13, 20, 22].

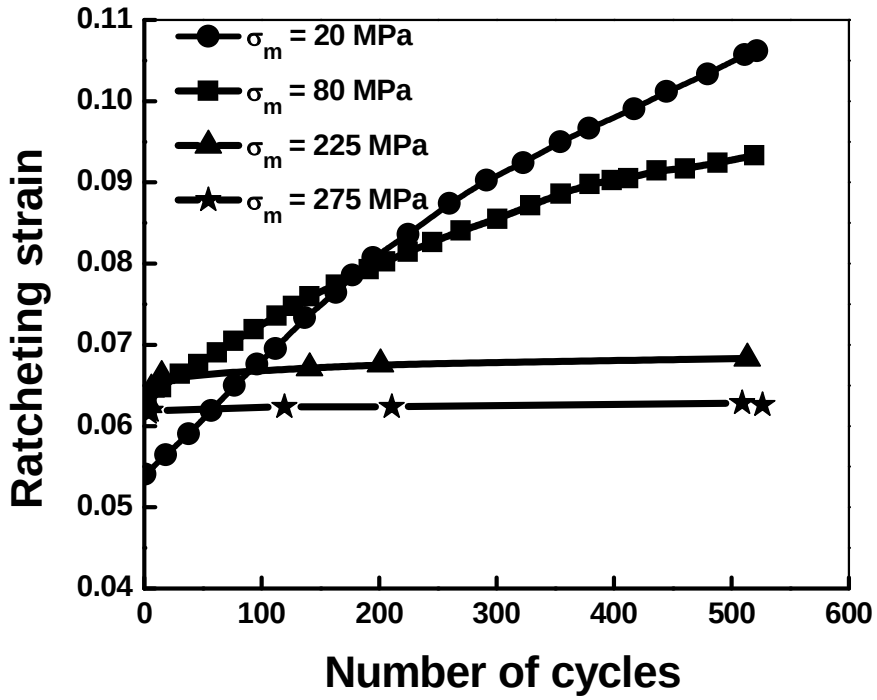

Fig. 2.7: Effect of mean stress on accumulation of ratcheting strain (following [11]).

However, it may be stated that the extent to which accumulation of strain occurs depends on the type of other stress parameters like maximum stress (σ_{max}), stress amplitude (σ_a), stress ratio (R) etc. It is reported for constant maximum stress conditions that the ratcheting strain accumulation decreases if mean stress increases as shown in Fig. 2.7. Chen et al. [7] have shown that for a lead-tin solder material, accumulation of strain increases with increase in mean stress at constant stress amplitude. The results of Chen et al. [7] are shown in Fig. 2.8 which indicates that the rate of strain accumulation decreases on the increase or decrease in the magnitude of mean stress. Kang [8] has studied uniaxial ratcheting behaviour of SiC_p-6061Al composites. He has also shown that strain accumulation of the composite increases with increasing mean stress at constant stress amplitude.

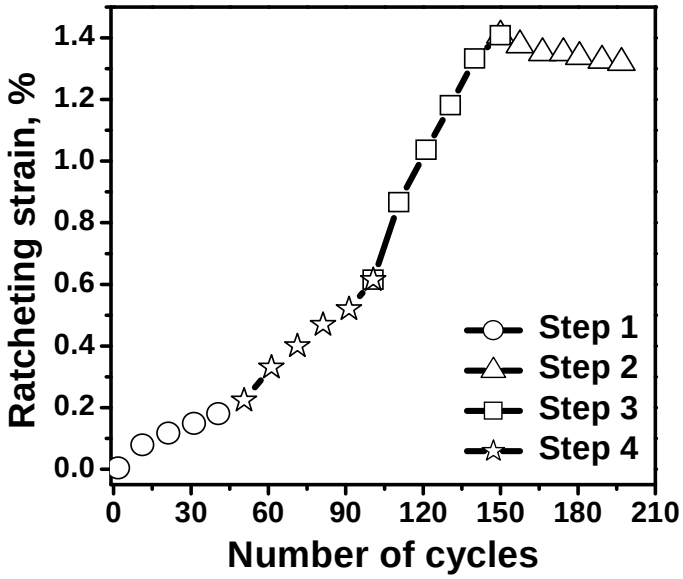

Fig. 2.8: Strain accumulation due to multi-step loading with variation of mean stress (following [8]).

2.5.2 Effect of maximum stress

Feaugas and Gaudin [11] have studied the effect of σ_{max} on ratcheting behaviour of AISI 316 stainless steel. It can be observed from their investigation results that when σ_m is constant, accumulation of ratcheting strain increases with increasing σ_{max} as shown in Fig. 2.9. The accumulation of strain due to ratcheting has been compared with static creep strain (i.e. creep at room temperature). These investigators reported that there exist two domains in a plot of strain rate, $d\varepsilon/dt$ *vs.* σ_{max}. The ratcheting strain rate ($d\varepsilon_r/dt$) is lower than the static creep rate ($d\varepsilon_c/dt$) up to a stress level; this particular stress level is chosen as the threshold for ratcheting strain. There is cyclic creep retardation (CCR) zone below the threshold level and above that is cyclic creep acceleration (CCA) zone. These phenomena are illustrated in Fig. 2.10.

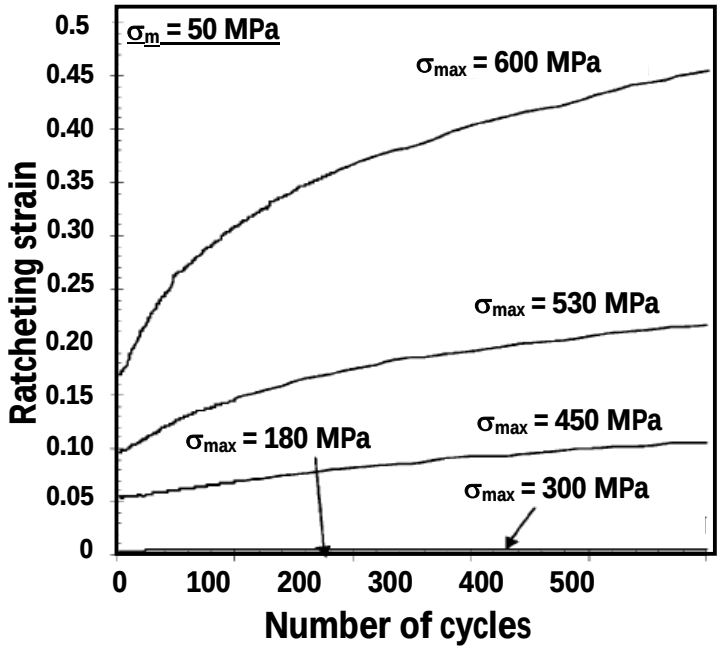

Fig. 2.9: Effect of maximum stress on accumulation of ratcheting strain (following [11]).

The transition from CCA to CCR depends on the stacking fault energy of materials. The magnitude of σ_{th} decreases as a function of $\gamma/\mu b$, where μ is shear modulus and b is Burgers vector.

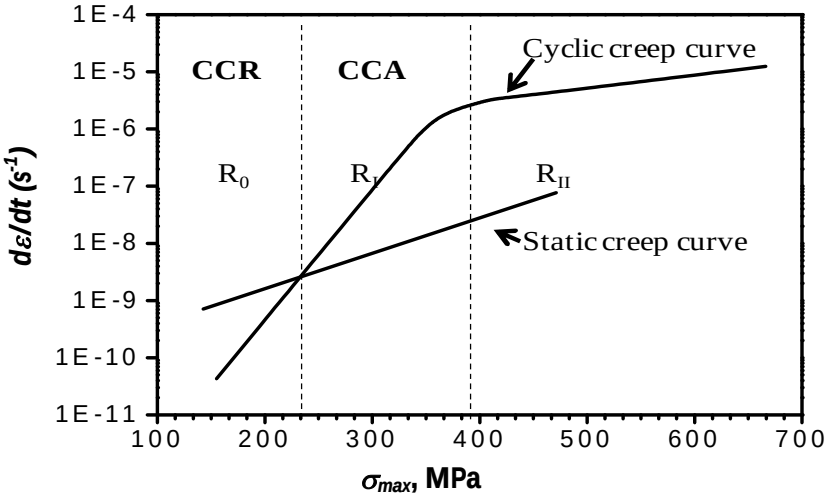

Fig. 2.10: The concept of threshold stress for cyclic creep (following [11]).

2.5.3 Effect of stress ratio

A few investigators [9] have examined the effect of stress ratio ($R = \sigma_{min}/\sigma_{max}$) on the nature of accumulation of ratcheting strain. Gupta et al. [9] have reported for ratcheting to occur in case of SA 333 group 6 piping steel, the stress ratio needs to be sufficiently negative. There have not been observed anyratcheting strain accumulation for $R = 0$ and $R = -0.25$ by this group of researchers, while there has been a significant accumulation of ratcheting strain for this material for R values of -0.5 and -0.75. It has also been reported that stress rate has considerable influence on the ratcheting response for negative stress ratios less than -0.25. Accumulation of ratcheting strain occurs at a faster rate when the applied stress rate is low (5 and 10 MPa/s) as compared to that at stress rates of 100 and 1000 MPa/s.

2.5.4 Effect of temperature

It is familiar that mechanical behaviour of materials is different at elevated temperatures than their behaviour at room temperature [24, 25]. Thus, ratcheting behaviour is also expected to get influenced by temperatures; which arouse interests in a few researchers [13, 22, 3]. The nature of strain accumulation has been investigated by Kang et al. [13, 22] at elevated temperatures for stainless steel. The experiments on ratcheting have been conducted by these authors at different temperatures as well as with stepwise increase in mean stress during cyclic loading. It is seen in the reports by Kang et al. states that the nature of accumulation of ratcheting strain in SS 304 at RT and at 573 K is similar. The ratcheting strain rate at each loading train decreases to almost zero after a few cycles and with increase in mean stress, ε_r increases at these temperatures. But at 973 K, ε_r increases with mean stress at a higher rate for this material, as shown in Fig. 2.11.

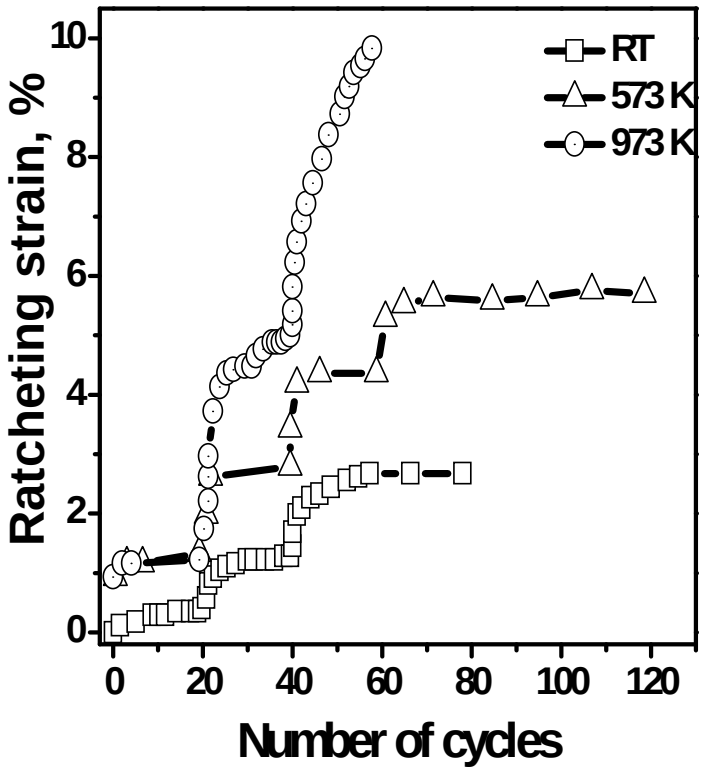

Fig. 2.11: Effect of temperature on accumulation of ratcheting strain (following [13]).

It can be clearly observed that the effect of mean stress is significant at elevated temperature on ratcheting behaviour of SS 304. Liu et al. [3] have examined the effect of temperature from sub-ambient to elevated temperatures on ratcheting behaviour of a polymeric material (poly methyl methacrylate). The nature of strain accumulation is illustrated in Fig. 2.12(a) and 2.12(b) respectively for this material at lower and higher temperature regimes. It can be observed that accumulation of strain increases with increasing temperature as well as with increasing maximum stress.

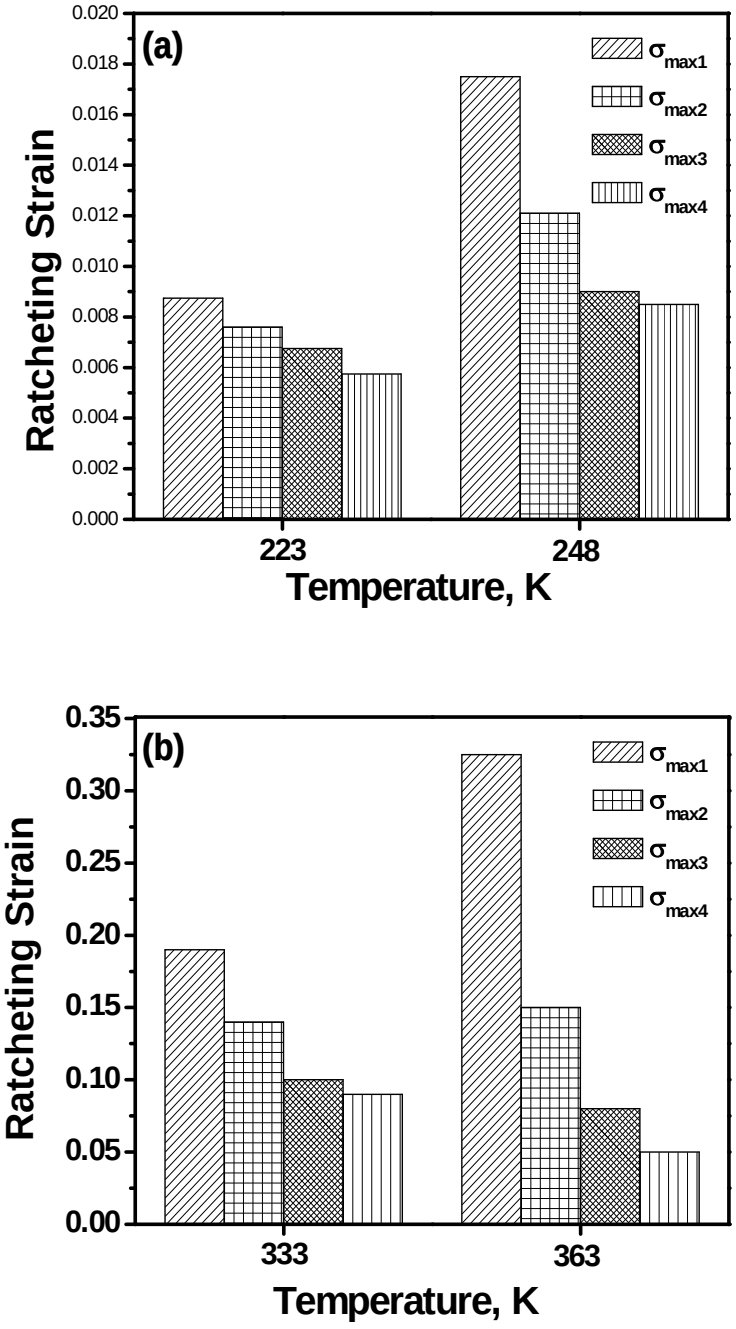

Fig. 2.12: Effect of temperature on accumulation of ratcheting strain: (a) below room temperature, (b) above room temperature. Here, $\sigma_{max1}>\sigma_{max2}>\sigma_{max3}>\sigma_{max4}$. (Following [3]).

2.5.5 Material dependence

Based on the nature of materials like whether they are cyclically hardenable or softenable, these materials may behave differently under symmetric cyclic loading [25, 26]. The characteristics of cyclically softenable materials inherently indicate that these materials get softened during cyclic loading; as a result of which during strain-controlled fatigue test, less stress is required to deform with increasing number of cycles. On the other half for cyclically hardenable materials, the required stress increases with increased number of cycles. If stress-controlled fatigue tests are performed, for cyclically softenable materials, material accumulates increased strain with number of cycles and strain accumulation decreases with number of cycles for cyclically hardenable materials. In both the cases, after about 100 cycles of loading, a stable hysteresis loop is observed due to attainment of some steady state.

It is thus obvious that accumulation of strain of a material significantly depends on the nature of the material. It is dependent on the cyclic hardening/softening features of the materials and cyclic loading conditions because ratcheting is a process of continued accumulation of plastic strain, under stress-controlled asymmetric cyclic loading.

2.6 Molecular Dynamics Simulation

Molecular dynamics (MD) simulation is a computer based simulation of the movements of atoms and molecules which are allowed to interact for a period of time. Generally, the trajectories of atoms and molecules are determined by solving the Newton's equations of motion for a system of interacting particles [19], where forces among particles and potential energy are defined by force fields of molecular mechanics. These simulations can be used to determine macroscopic thermodynamic properties of the system. MD simulation is also known as "statistical mechanics

by numbers" and "Laplace's vision of Newtonian mechanics" as it predicts the future by animatingthe forces of nature and providing an insight into motion of molecules on an atomic scale. A molecular dynamics simulation requires a description of the particles in the simulation which will interact. Potentials may be defined at many levels of physical accuracy; those most commonly used in chemistry are based on molecular mechanics and personify a classical treatment of particle-particle interactions that can generate structural and conformational changes but usually cannot produce chemical reactions.

In theoretical physics and applied mathematics, Molecular Dynamics is a part of the research area of dynamical systems; atomic and molecular physics and statistical mechanics. MD can also be said to be a case of discrete element method (DEM) where particles have a spherical shape.Since big molecular systems comprise of a large number of particles, it is impossible to find the properties of these complex systems analytically; MD simulation finds a solution to this problem by using numerical analysis. However, lengthy MD simulations are ill-conditioned mathematically, producingcollective errors in numerical integrations that can be reduced byappropriate selection of parameters, but cannot be eliminated entirely.

2.7 Advantages of using Molecular Dynamics Simulation

Earlier investigators have studied the properties of nanoscale copper under static loading while very few studies have been conducted to test the effect of cyclic loading as it consumes a lot of time when the experiment is conducted in real life. However, conducting fatigue experiments at high temperature is really a challenge and needs prolonged duration of time. Hence many molecular simulation studies have come into picture to predict the fatigue behavior of materials

at varying temperatures. Using molecular dynamics simulation, 100% pure copper can be obtained which is practically impossible. Moreover, testing can be carried out at sub-ambient, ambient and elevated temperatures at the same time, facilities for which are not available in our labs.

2.8 Review of the current problem

There are numerous investigations related to fatigue behaviour of materials under symmetric cyclic loading. But in contrast, very limited investigations are on asymmetric loading conditions; therefore this demands attention of the researchers to gather information on ratcheting behaviour of materials. The effects of various test parameters like mean stress, maximum stress, stress ratio, temperature etc. on ratcheting behaviour of materials have been inspected, and most of these investigations mostly addresses the issue in terms of mechanics of materials.

The existing reports provide information related to ratcheting behaviour of materials on the following: (i) ratcheting strain accumulation is a function of σ_m, σ_{max}, R, T etc., (ii) ratcheting strain accumulation depends on the nature of the investigated material based on their characteristic cyclic hardenability or softenability. Although different systems of material have been examined for the study of their ratcheting behaviour but still there is not systematic analysis on materials with varying characteristics. Due to this there is great necessity to investigate about the effect of different loading parameters on the nature of ratcheting strain accumulation for materials of different crystal structures. In addition, due to accumulation of ratcheting strain there can be cyclic hardening or softening of a material which can alter its mechanical properties. However, in earlier reports this hypothesis has not been verified.

Works through mathematical analysis are done to understand the ratcheting behaviour of materials. But there is lack of investigations on ratcheting behaviour at atomistic level therefore an attempt has been made to gain some knowledge on ratcheting behaviour of materials through MD simulations.

This investigation, in brief, attempts to understand:

(i) tensile behaviour of the investigated material i.e. nanoscale copper at various temperatures;

(ii) the nature of strain accumulation due to ratcheting at various temperatures and stress ratios in nanoscale copper.

CHAPTER 3

Molecular Dynamics Simulation using LAMMPS

OUTLINE

Introduction

Simulation Procedure

Simulation Parameters

Sample Configuration

Tensile Test

- **(a) Input file for obtaining equilibrated 3D-crystal lattice.**
- **(b) Input file for tensile testing of a previously equilibrated crystal**

Ratcheting Test

- **(a) Effect of Stress Ratio**
- **(b) Effect of Temperature**
- **(c) Input file for performing ratcheting test on pure copper of box size [30x65x30] previously equilibrated**

3.1. Introduction:

In this investigation, Molecular Dynamics simulation of nano-scale copper has been done using LAMMPS (Large-scale Atomic/Molecular Massively Parallel Simulator)[19]. LAMMPS is a classical molecular dynamics simulation code designed to run efficiently on parallel computers. It is an open-source code that models an ensemble of particles in a liquid, solid, or gaseous state. It can model atomic, polymeric, metallic, granular, and coarse-grained systems using a variety of force fields and boundary conditions.

LAMMPS integrates Newton's equations of motion for collections of molecules, atoms, or macroscopic particles which interact by short- or long-range forces with a variety of initial and/or boundary conditions. For computational efficiency, LAMMPS uses neighbor lists (optimized for systems with particles that are repulsive at short distances, so that the local density of particles never becomes too large) to keep track of nearby particles. On parallel machines, to partition the simulation domain into small 3d sub-domains, LAMMPS uses spatial-decomposition techniques.

A LAMMPS input script has 4 parts:

1. Initialization
2. Atom definition
3. Settings
4. Run a simulation

LAMMPS executes commands from an input script (text file), reading one line at a time. It exits when the input script ends. Every command causes LAMMPS to perform an action; it can read in a file, set an internal variable, or run a simulation. Generally, the ordering of commands in an input script is insignificant.

However the following points should be taken care of:

(1) LAMMPS reads the input script one line at a time and each command takes effect immediately when it is read, not after the complete text file is read.

(2) A few commands are valid only when they follow other commands. A group Command can only be used after the atoms are defined.

(3) Sometimes a command X may use values set by command Y. This means command X must follow command Y in the input script if it is to have the required effect.

3.2. Simulation procedure

Recently, Murali et al [21] have done atomic scale studies on the fracture behavior of $Cu_{50}Zr_{50}$ alloy system coded in LAMMPS in which they used embedded-atom method (EAM) potentials for modelling the atomic interactions.

In our simulations we used EAM FS (Finnis-Sinclair) potential developed by Mendelev et al [23] and it is a valid potential. In the EAM, the total energy of an *N*- atom system is represented in the following equation:

$$E_{\text{tot}} = \sum_i F_i(\rho_i) + \frac{1}{2} \sum_{\substack{i,\ j \\ i \neq j}} \varphi_{i,\ j}(r_{i,\ j}) \qquad \textbf{(3.1)}$$

where $\varphi_{i,j}(r_{i,j})$ is a short range pair potential between atom i and j with the separation distance $r_{i,j}$, $F_i(\rho_i)$ is the embedding energy of atom i with the electron density ρ_i due to all its neighbors is expressed below:

$$\rho_i = \sum_{j \neq i} f_j(r_{ij}) \qquad \textbf{(3.2)}$$

In Finnis/Sinclair model the total energy of an atom is represented by the following equation:

$$E_i = F_\alpha\left(\sum_{j \neq i} \rho_{\alpha,\beta}(r_{i,j})\right) + \frac{1}{2}\sum_{j \neq i} \varphi_{\alpha,\beta}(r_{i,j}) \qquad \textbf{(3.3)}$$

where ρ the electron density is a functional specific to the atomic types of both atoms *i* and *j* so that different elements can contribute differently to the total electron density at an atomic site depending on the identity of the element at that atomic site and alpha and beta are the element types of atom *i* and *j*. The initial amorphous structures for simulation were obtained using NPT ensemble with zero applied pressure. Timestep is equal to 0.002 ps. Equations of motion are numerically integrated using velocity-Verlet algorithm.

3.3. Simulation Parameters:

LAMMPS requires as input a list of initial atom coordinates and types, molecular topology information, and force-field coefficients assigned to all atoms and bonds.It has potentials for soft materials viz. biomolecules, polymers; solid-state materials viz. metals, semiconductors and coarse-grained or mesoscopic systems.VMD is a simple and fast visualizer provided with the LAMMPS package which creates xyz projection views of atomic coordinates and animates them. Through VMD we can visualize the changes taking place step by step in the simulation.

While writing the simulation input file code, variables like potential file, lattice parameters, maximum and minimum stress, temperature, number of cycles and number of iterations are changed. These parameters govern the simulation conditions and environment. For atomic systems LAMMPS provides a create_atoms command which places atoms on solid-state lattices

(fcc, bcc, user-defined, etc). Assigning small numbers of force field coefficients can be done via the pair coeff, bond coeff, angle coeff, etc commands.

Simulation box size, timestep and total duration must be adjusted such that the calculation can finish within a reasonable time period. However, the simulations should be made as long as it can be so as to match the time scales of the natural processes being studied. In other words, to make statistically valid conclusions, the time span of the simulation should match the kinetics of the natural process. The timestep should be small enough so as to avoid discretization errors (i.e.it must be smaller than the frequency of fastest vibrations of the system). The simulation box size must be large enough to avoid boundary condition artifacts. Boundary conditions are often treated by choosing fixed values at the edges (which may cause artifacts), or by employing periodic boundary conditions in which one side of the simulation loops back to the opposite side, imitating a bulk phase.

NVE (Micro-canonical ensemble): In NVE ensemble, the system undergoes an adiabatic process and is isolated from changes in moles (N), volume (V) and energy (E).

NVT (Canonical ensemble): In NVT, also sometimes called as constant temperature molecular dynamics (CTMD), moles (N), volume (V) and temperature (T) are conserved and the energy of endothermic and exothermic processes is exchanged with a thermostat.

NPT (Isothermal–isobaric) ensemble: In NPT ensemble, moles (N), pressure (P) and temperature (T) are conserved. A barostat is also needed along with a thermostat. It corresponds to laboratory conditions with a flask open to ambient temperature and pressure.

3.4. Sample Configuration:

The initial configuration of atomic assembly for various molecular dynamics simulations is shown in Fig. 1. Both tensile and fatigue simulations were performed using this type of sample configuration. The assembly contains three regions; grip region at the opposite ends which is composed of immobile atoms and tension/tension-compression region which include the mobile atoms. Tensile and uniaxial fatigue loading were carried out in the y-direction, as indicated in Fig. 1. The periodic boundary condition was imposed on the x and z axis and the material was free to be strained in the y-direction only.

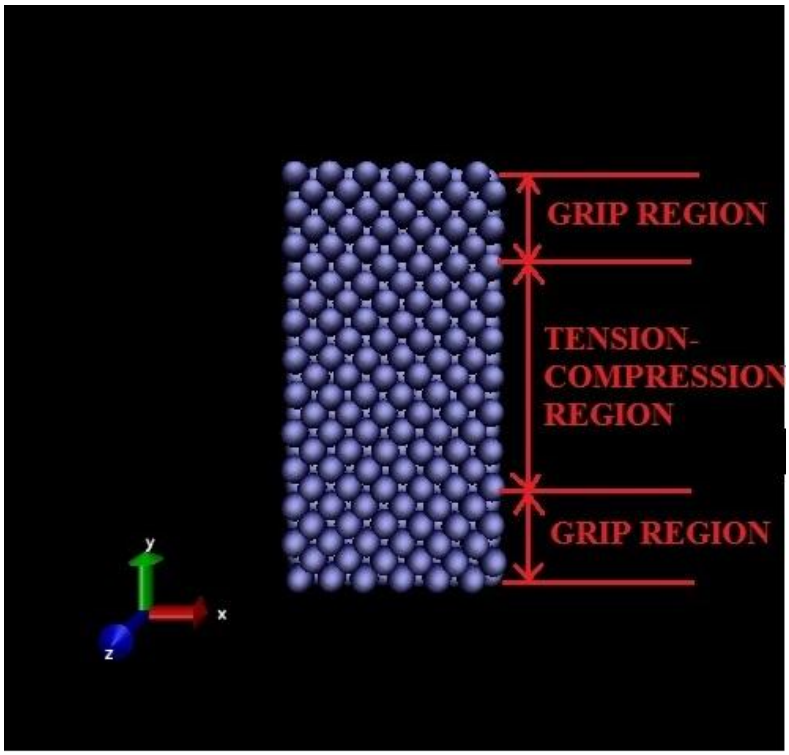

Fig.3.1: VMD snapshot of the sample undergoing simulation.

3.5. Tensile Test:

It is considered for any MD simulation study that an energy minimisation of the system is required before performing the actual simulation studies. Through iterative adjustment of atom coordinates, the configuration attains a position of minimum local potential energy [19]. The configuration used for tensile testing was therefore equilibrated at room temperature using the method described above. The tensile test was then carried out at three different temperatures viz. 100 K, 300 K and 500 K with the parameters as mentioned in Table 1. The strain in the y-direction was calculated using the following equation:

$$e = \text{loading rate} * \text{time} \qquad (3.4)$$

where time = timestep * step number (timestep = 0.001 ps)

Loading rate = 0.1/ps

To understand the effect of specimen design, simulations were carried out at different box dimensions [Table 1] and the typical outcome obtained was plotted in the form of stress-strain curves.

Table 1: Size and Dimensions of Sample Undergoing Simulation

Sl. No.	Box Dimensions	Total Number of Atoms	Number of Mobile Atoms
1.	40 x 100 x 40	14812	9349
2.	32 x 68 x 32	6156	4623
3.	30 x 65 x 30	5347	3868
4.	20 x 50 x 20	2016	1243

3.5.1. Input file for obtaining equilibrated 3D-crystal lattice using LAMMPS:

```
units           metal      …→ determines units of all quantities used in the input file
echo            both       …→ echoes each input script command to both log file and screen
atom_style      atomic
dimension       3
boundary        p p p      …→periodic boundary condition

region          box block 0 30 0 65 0 30  units box    →defines a geometric region of space
create_box      1 box           .....→creates a simulation box in the specified region

lattice         fcc 3.61        ……..→lattice type and lattice parameter
region          cu block 0 30 0 65 0 30 units box
create_atoms    1 region cu units box …→ creates copper atoms in the simulation box

timestep        0.002           ……→ sets the timestep for subsequent simulations
pair_style      eam/alloy
pair_coeff      * * Cu_zhou.eam.alloy Cu   ……→specifies the potential file used

# Energy Minimization
Minimize        1.0e-4 1.0e-5 10000 10000

thermo          10                                  →computes and prints thermodynamic
                                                        data after every 10 timesteps

thermo_style    custom step temp vol press etotal pe ke →specifies content of thermodynamic
                                                        data to be printed in screen &
                                                        log file

dump            1 all atom 100 Cu_crystal_3d_s_dump_EQUILIBRATED.lammpstrj
                                  ..…→dumps a snapshot of atom quantities every 100 timesteps
                                      to the specified file

dump_modify     1 scale no …→modifies parameters of previously defined dump command.
                                      A value of scale 'no' means atom coordinates are written in
                                      absolute distance units.

log             logCu_crystal_3d_s_EQUILIBRATED.data
                                  … →closes the current log file, opens a new log file, and begins logging
                                      information to it
```

velocity all create 300 873847 rot yes mom yes dist Gaussian **…→sets the velocity of a group of atoms**

#fixes

fix 1 all npt temp 300 300 0.1 iso 0.0 0.0 0.1 **→temp and pressure conserved**

run 1000 **… → program is run for 1000 iterations**

unfix 1 **… →deletes the previously defined fix 1**

3.5.2. Input file for tensile testing of a previously equilibrated crystal:

 # 3d tensile simulation JP4review

```
units           metal
boundary        p p p
atom_style      atomic
echo            both

read_data       EQUILIBRATED_CRYSTAL_file.txt
```
→reads the data file containing the atom positions of the equilibrated crystal in the specified file

```
timestep        0.001
pair_style      eam/alloy
pair_coeff      * * Cu_zhou.eam.alloy Cu

dump            1 all atom 100 dump.JP4_tensile_ 10^11s_1_70%strain_allatoms.lammpstrj
log             log5050_JP4_review_10^11s-1_70%strain_f1_allatoms.dat

velocity        all create 700 482748 rot yes mom yes dist gaussian

fix             1 all deform 1 y erate 0.1
```
….→strain rate of 0.1 sec^{-1} is applied in y direction

```
fix             2 all npt temp 700.0 700.0 10.0 x 0 0 10.0 z 0 0 10.0 dilate all
```
…→all atoms rescaled to new positions while temp and pressure is conserved

```
fix             3 all temp/rescale 10 700 700 0.05 1.0
```
→Resets the temp of atoms to 700K by rescaling velocities after every 10 steps

compute 1 all stress/atom **…→ computes the symmetric per-atom stress tensor for each atom in a group.**

compute 2 all temp **… → computes the temp of a group of atoms**

dump 2 all custom 1 dump.stress_atom_Jp4_review_10^11s-1_70%strain_f1_allatoms type x y z c_1[1] c_1[2] c_1[3] c_1[4] c_1[5] c_1[6]
→dumps atom type; x,y,z coordinates; 6 stress tensors computed in 1 to an array of 6 elements

compute 3 all reduce sum c_1[2] **→reduces vector quantities of all stress tensors in y-direction and adds all the quantities to a single scalar value**

variable stress equal c_3/(3*160000) **→assigns a value to the variable name stress**
variable stress_GPa equal v_stress/10000 **→converts the stress calculated to GPa**

thermo 1

thermo_style custom step temp press voletotal c_2 v_stressv_stress_GPa

run 7000 **… → number of iterations is given so as to give 40% strain to the material**

3.6. Ratcheting Test:

To find the variation of Ratcheting strain with number of cycles, low cycle asymmetric fatigue loading of pure Copper has been done using Molecular Dynamic simulation. In this study, ratcheting strain is being defined as the average of maximum and minimum strains at a particular cycle, following few other reported definitions. In this study, ratcheting strain has been calculated as:

$$\textbf{Ratcheting strain\%} = \left[\frac{\left(Y_{hi} + |Y_{lo}|\right) - L}{2L}\right] * 100 \qquad \textbf{(3.5)}$$

where, Y_{hi} and Y_{lo} are the elongated crystal coordinates in the positive and negative y-direction respectively;

L is the initial length of the crystal in the y-direction.

Stress values for practical experiments are much lesser than that required for simulations. While simulating, we take 100% pure sample which is impossible to obtain practically. The imperfections and micro-cracks in the sample while conducting real-life experiments acts as regions of high stress concentrations where failure occurs at much lower levels of applied stresses. Thus as practical cohesive strength is much lower than the ultimate tensile strength as also explained by Griffith's criterion, stress values taken in ratcheting simulation is very high.

3.6.1. Effect of Stress Ratio

Simulation studies related to ratcheting deformation has been carried out under various stress ratios (R). The R values have been chosen in such a manner that all the tests comprise to positive mean stress conditions. The employed R values are summarized in Table 2.

Table 2: Parameters to study the effect of R-ratio in ratcheting strain

Sl. No.	R-ratio	σ_{max}(GPa)	σ_{min}(GPa)	Temperature	Size of Box
1.	-0.2	-14.5	2.9	300 K	40 x 100 x 40
2.	-0.4	-14.5	5.8		
3.	-0.6	-14.5	8.7		

Practically Copper breaks at 210MPa (from ASM Handbook) but while simulation the material withstands much higher value. This is in accordance with the previous explanation of using a defect-free crystal in simulations.

From the results obtained from simulations, a graph was plotted for better understanding of the effect of stress-ratio in ratcheting tests.

3.6.2. Effect of Temperature

In order to study the effect of temperature on the ratcheting behavior, simulations were carried out at a range of temperatures below the melting point of the material (melting point of copper is 1080^{o}C (1353K)).

To show dependence of temperature on ratcheting strain, simulations on uniaxial ratcheting have been conducted in two phases at temperatures viz. 100 K, 300 K, 500 K and 700 K. For 1st phase, the maximum stress ($\sigma_{max)}$ is taken as 90% of the UTS value (at every temperature) with constant stress ratio (R) = -0.2. Fatigue testing simulations were performed and ratcheting strain at different temperatures was calculated for 10 cycles. For 2nd phase, fatigue testing simulations were carried out at a fixed value of σ_{max} and σ_{min} for 50 cycles.

Table 3: Parameters for Ratcheting test to study the influence of temperature (1st phase)

Sl. No.	Box Dimensions	Temperature(K)	UTS (GPa)	σ_{max} (GPa)
1	30 x 65 x 30	100	1.131	1.00
2		300	0.83	0.70
3		500	0.502	0.40
4		700	0.119	0.10

3.6.3. Input file for simulation of ratcheting test on pure copper of box size [30 65 30] previously equilibrated

 # Ratcheting simulations of pure Cu at R= -0.2 at 300 K for 10 cycles [1st phase]

```
units           metal
boundary        p p p
atom_style      atomic
echo            both

#take sample created at 300 K
read_data       EQUILIBRATED_CRYSTAL_file.txt   →reads the data file containing the
                                                atom positions of the equilibrated
                                                crystal in the specified file
timestep        0.002

pair_style      eam/alloy
pair_coeff      * * Cu_zhou.eam.alloy Cu

# mobile zone
region          1 block 0 30 0 10 0 30 units box  … →defines a geometric region of space
                                                  around the specified xyz coordinates
region          2 block 0 30 55 65 0 30 units box

group           lower region 1                  …→identifies a collection of atoms in
                                                  region1 as a group named 'lower'
group           upper region 2

group           boundary union lower upper      …→group 'boundary' refers to the union
                                                  of 'upper' and 'lower' groups

group           mobile subtract all boundary    …→group 'mobile' identifies all atoms not
                                                  present in group 'boundary'
```

 # initializing velocities

velocity mobile create 300.0 873847 rot yes mom yes distgaussian

fix 2 boundary setforce 0.0 0.0 0.0 **→sets each component of force on each atom in group 'boundary' as 0,0,0**

compute 2 mobile temp **…→computes temperature of 'mobile' group**

thermo 100

thermo_style custom step temp yloyhietotal press pyy c_2

dump 2 all atom 1000 Cu_fatigue_LOOP_300k_2,1.dump_test.lammpstrj

→dumps a snapshot of all atom quantities every 1000 timesteps to the specified file

dump_modify 2 scale no

log logCu_fatigue_3d_LOOP_300k_2,1_test.data

dump 3 mobile atom 1000 Cu_fatigue_mobile_LOOP_300K.dump_test.lammpstrj

→dumps a snapshot of atom quantities in group 'mobile' every 1000 timesteps to the specified file

dump_modify 3 scale no

#fixes

fix 3 mobile nve **…→ Performs constant NVE integration to update position and velocity for atoms in the group 'mobile' each timestep**.

fix 4 mobile temp/rescale 100 300 300 0.05 1.0**→Resets the temp of atoms in 'mobile' group to 300K by rescaling velocities after every 100 timesteps**

 # loop is given below for the fix 5

label loop1**…→used for looping over a section of the input script**

#number of cycles=10

variable d loop 10 **→number of cycles=10. When the "d" variable has been incremented for the tenth time, it will cause the next jump command to be skipped.**

label loopstart

 # number of iterations in each cycle=10000*4=40000

variable a loop 4

variable s index 0 -145000 0 29000

variable e index -145000 0 29000 0

For the *index* style, one or more strings are specified. Initially, the 1st string is assigned to the variable. Each time a next command is used with the variable name, the next string is assigned.

fix 5 mobile press/berendsen y $s $e 100 dilate all

→Resets the pressure of 'mobile' by using a Berendsen barostat. Pressure varied from value of 's' to value of 'e' in y-direction.

run 10000**→Each variation from value in 's' to 'e' takes place in 10000 iterations**

#log log.$s-$e

next s

next e

next a

'next' is used with variables defined by the 'variable' command. It assigns the next value to the variable from the list of values defined for that variable by the variable command.

jump in.Cu_fatigue_loop_Dan.txt loopstart**→jumps to the label 'loopstart' where execution begins again with incremented value of 'a'**

next d

jump in.Cu_fatigue_loop_Dan.txt loop1

Chapter 4

Results and Discussion

OUTLINE

Tensile properties

(a) Effect of temperature on tensile behaviour

(b) Effect of specimen design

(c) Effect of temperature on UTS

Uniaxial ratcheting

(a) Effect of stress ratio (R)

(b) Effect of temperature

4.1. Tensile Properties:

The primary aim of this investigation is to study asymmetric fatigue behavior of nanoscale pure copper. Before conducting any test related to it, Molecular Dynamics simulations using LAMMPS were carried out to find tensile behaviour of the investigated material at various temperatures.

4.1.1. Effect of temperature on tensile behaviour

Simulations were carried out at different temperatures to study the effect of temperature on the tensile properties of nanoscale copper. The generated results from tensile simulations were analyzed and the data were plotted to generate the stress-strain curves of nanoscale copper at various temperatures (100K, 300K and 500K). Typical stress-strain curves are illustrated in the figures below:

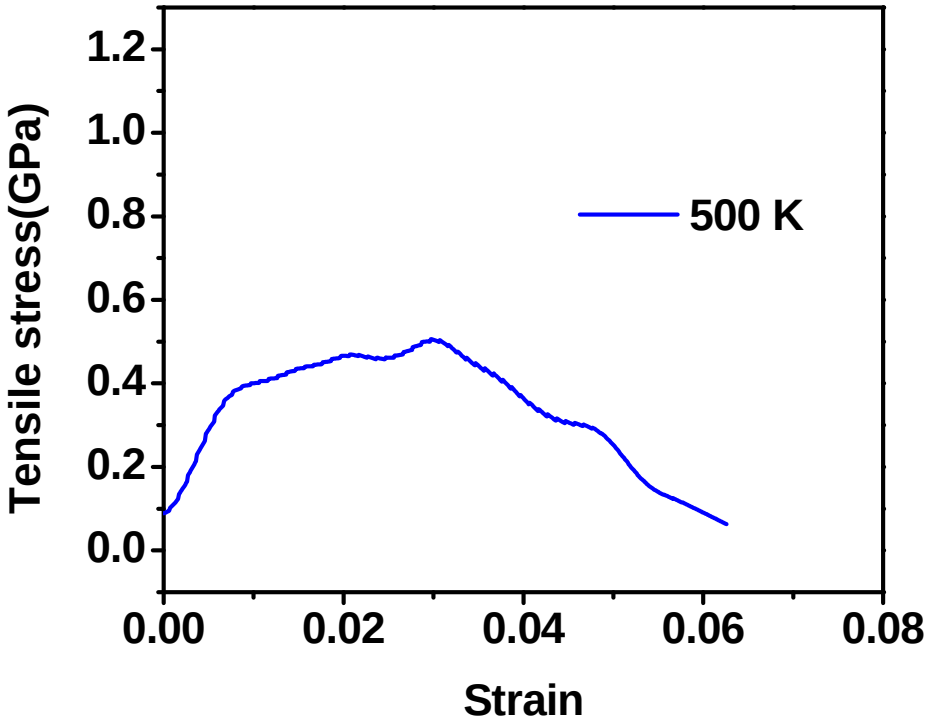

Fig. 4.1: Tensile stress vs. strain at 500 K.

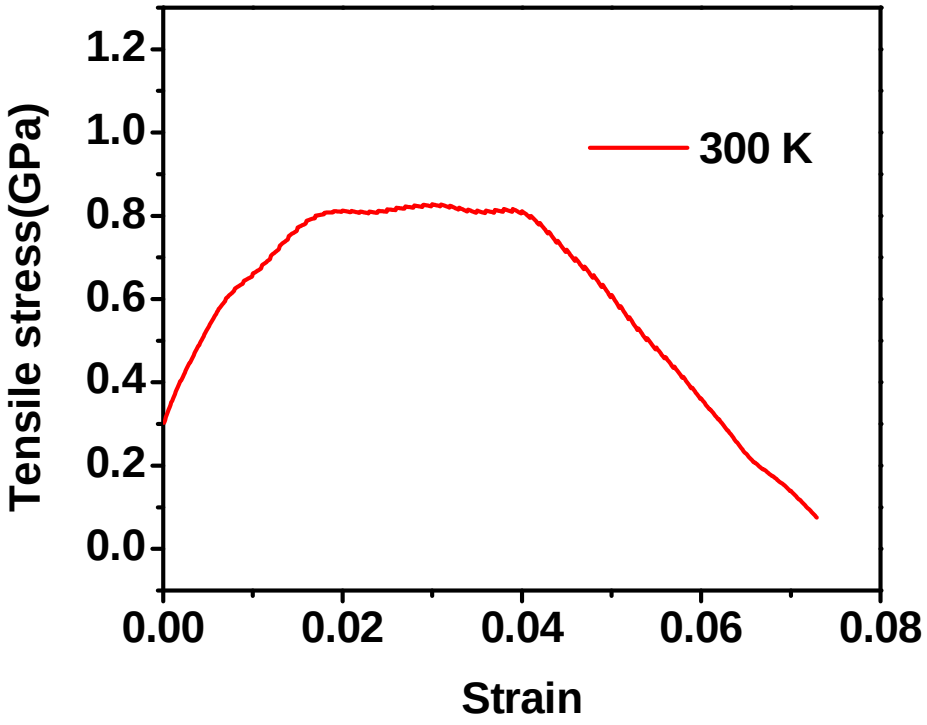

Fig. 4.2: Tensile stress vs. strain at 300 K.

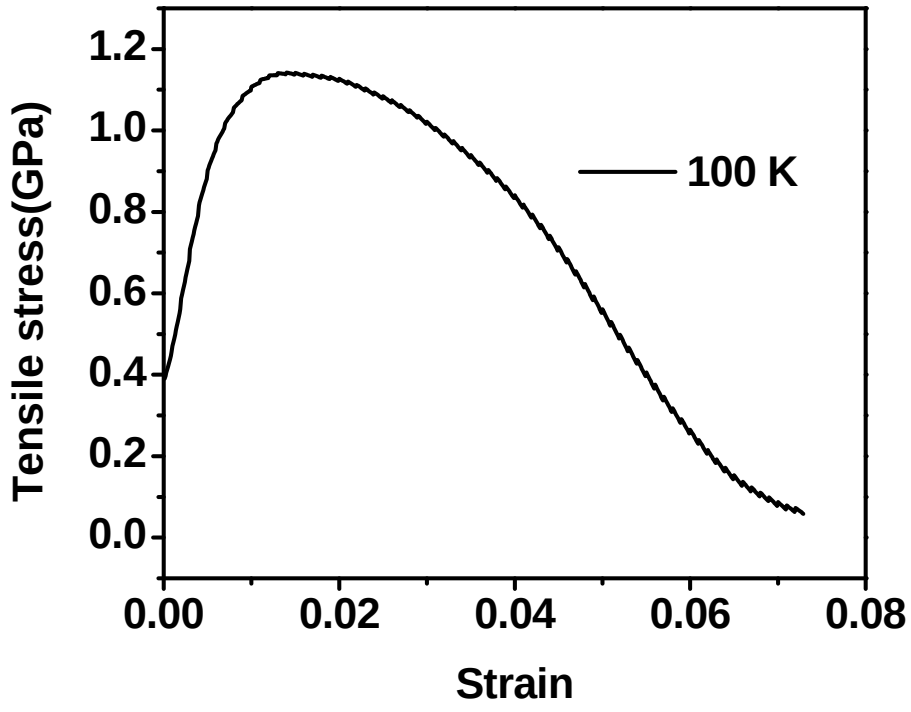

Fig. 4.3: Tensile stress vs. strain at 100 K.

This is well understood that strength of metallic materials decreases with increasing temperature [25, 26]. From the simulation results on nanoscale copper, similar results has been obtained. The stress-strain curves at 100 K, 300 K and 500 K when plotted in a single graph clearly indicate the effect of temperature as illustrated in Fig. 4.4.

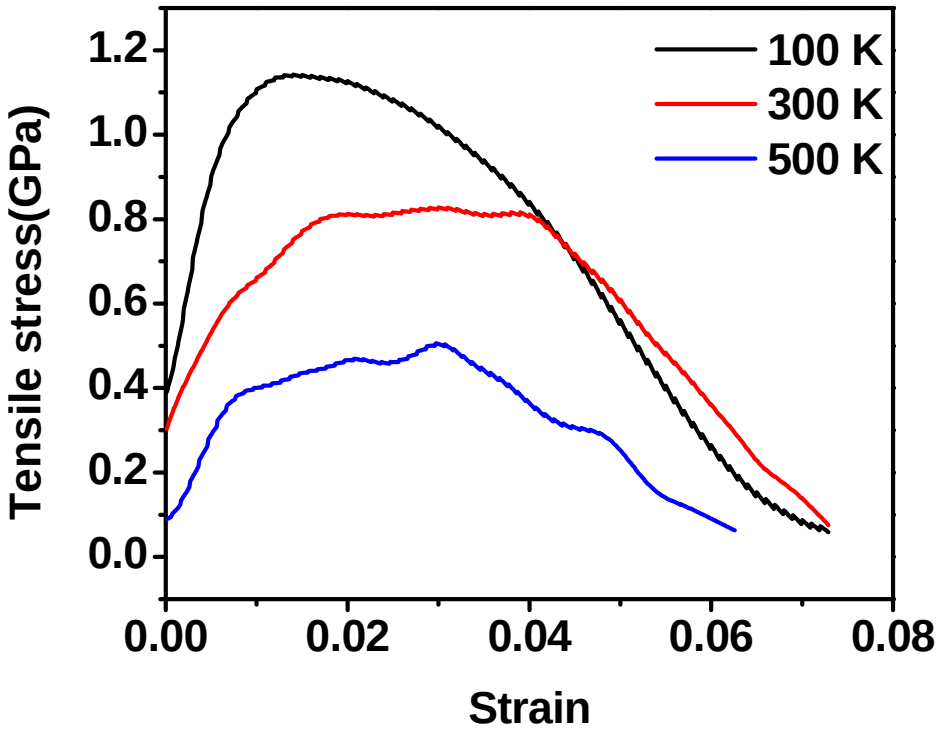

Fig. 4.4: Relationship between tensile stress and strain at various temperatures.

It can be seen from the figure above that with increase in temperature, the stress-strain curves dropped down, as expected. It is well known that flow stress decreases at higher temperatures; similar features can be observed from the current set of simulation studies.

4.1.2. Effect of specimen design

It can be expected that properties of nanoscale materials should vary based on number of atoms present in a cluster of atoms. This may be interpreted as the variations in specimen design. To understand the effect of specimen design, simulations were carried out at different box dimensions; these are mentioned in Table 1 (Chapter 3).Typical stress strain results obtained from these simulations was plotted which are illustrated in the figures below:

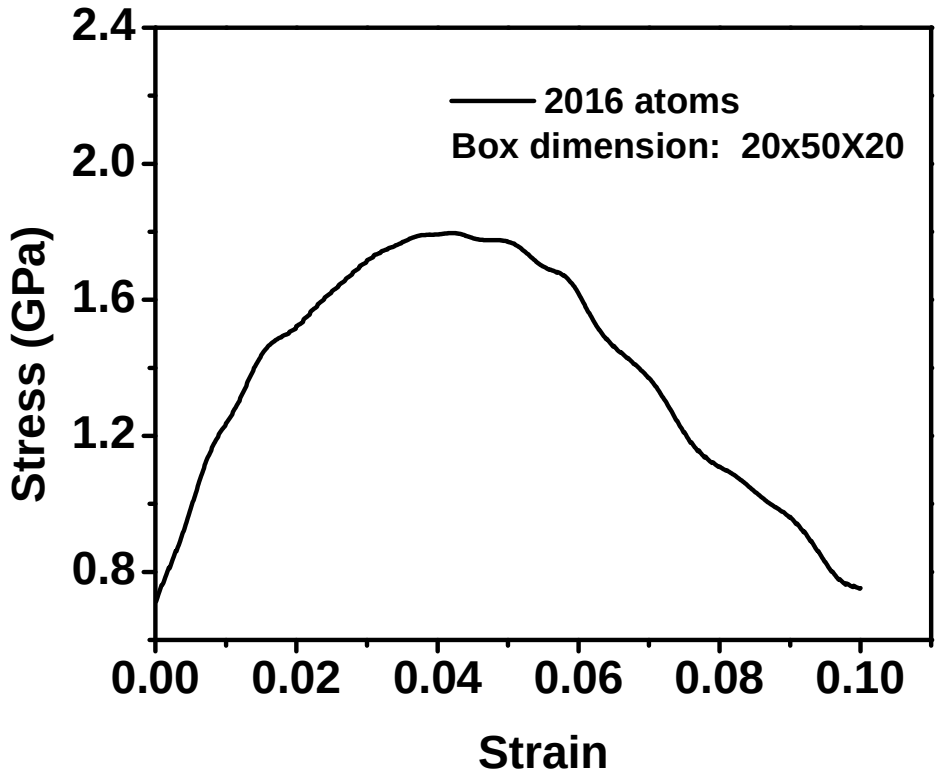

Fig. 4.5: Relationship between tensile stress and strain;

Box dimensions: 20 x 50 x 20

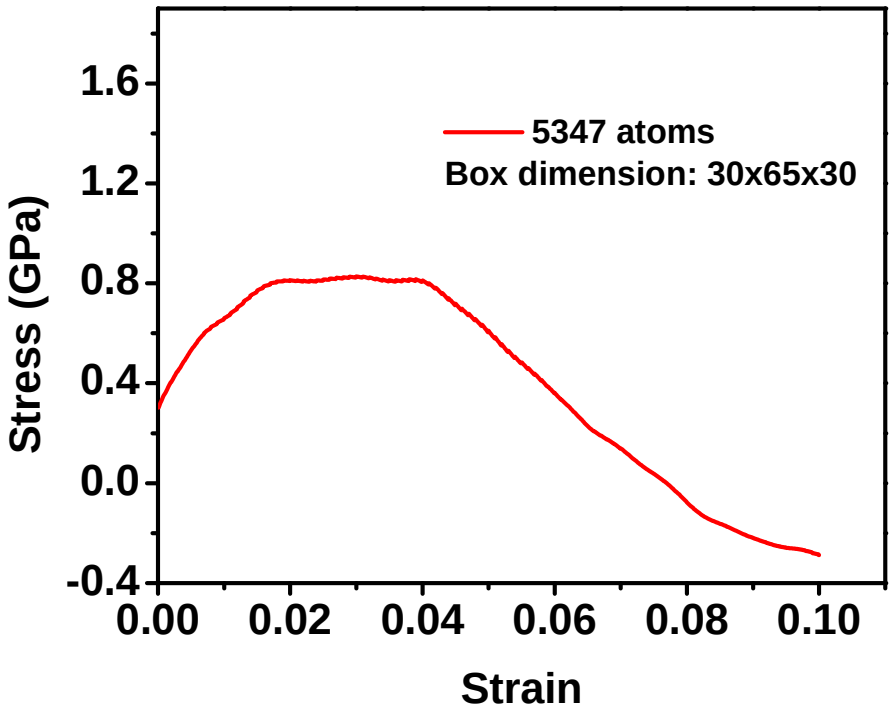

Fig. 4.6: Relationship between tensile stress and strain; Box dimensions: 30 x 65 x 30

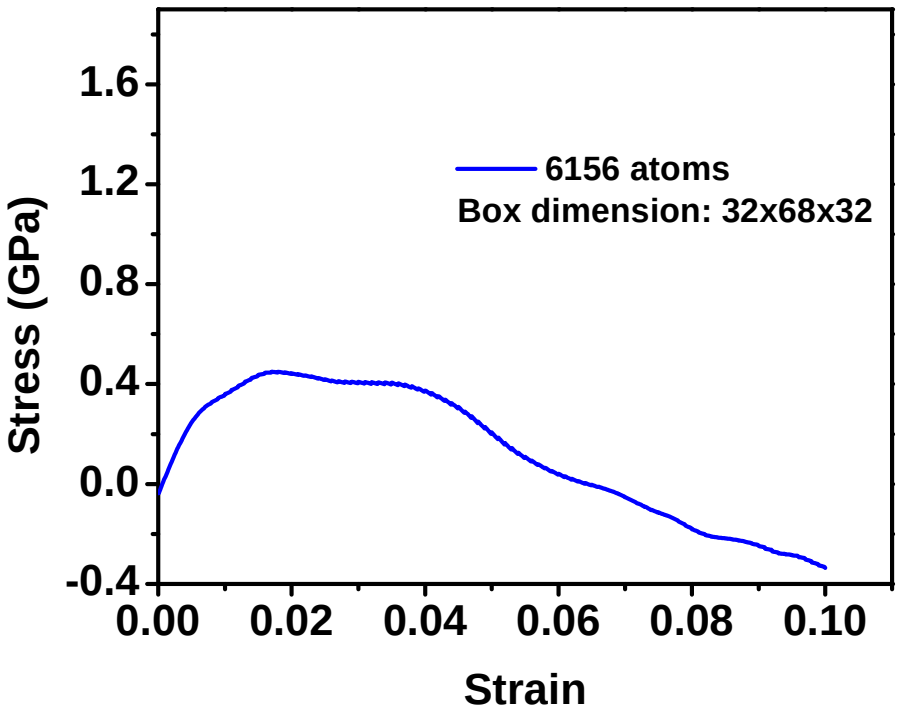

Fig. 4.7: Relationship between tensile stress and strain; Box dimensions: 32 x 68 x 32

In order to understand the effect of specimen design or box dimensions on the tensile stress-strain plots, a comparative study was made by plotting the above graphs in a singular plot. The variations are illustrated in Fig. 4.8.

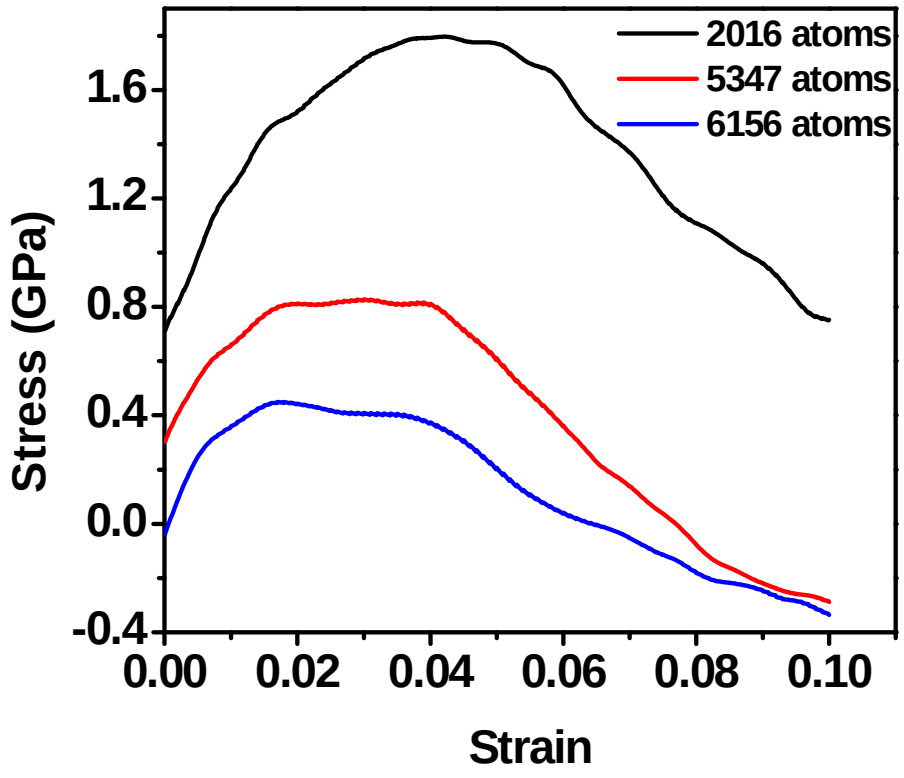

Fig. 4.8: Variation of stress-strain curve for different box dimensions.

It was seen that, at room temperature, materials with smaller box dimensions had a higher UTS as illustrated in Fig. 4.8. This is because in case of MD simulation, lower the number of atoms in the sample, more difficult it gets to strain the material; in other words, the strength of the sample is more in case of a sample with smaller box dimension (or lesser number of atoms).

It can be seen in Fig. 4.8 that temperature has considerable influence on the slope of the elastic region of the curve. The slope of the elastic region corresponds to the Young's modulus of the material. It can be observed that with increase in temperature, the slope of the curve decreases; this corresponds to decrease in Young's modulus of nanoscale copper.

4.1.3 Effect of temperature on ultimate tensile strength

For better understanding of the influence of temperature on the ultimate tensile strength (UTS) of nanoscale copper, simulations were carried out to study the tensile behavior at different temperatures.

The above simulations were carried out at different box dimensions. The value of UTS was calculated in each simulation and plotted as shown in the figures below. The UTS was seen to decrease with increase in temperature.

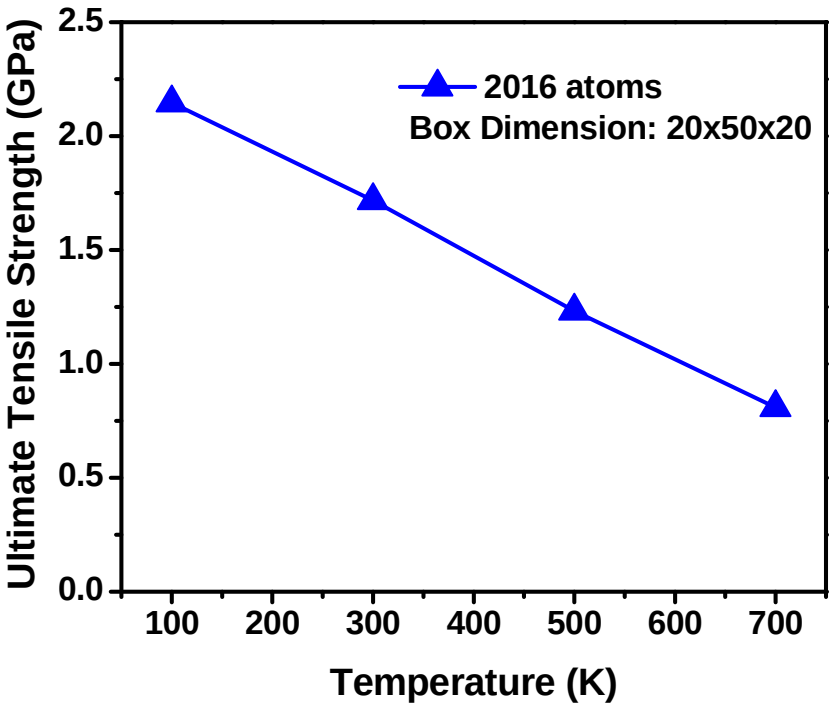

Fig. 4.9: Ultimate Tensile Strength vs. Temperature; Box Dimensions: 20 x 50 x 20

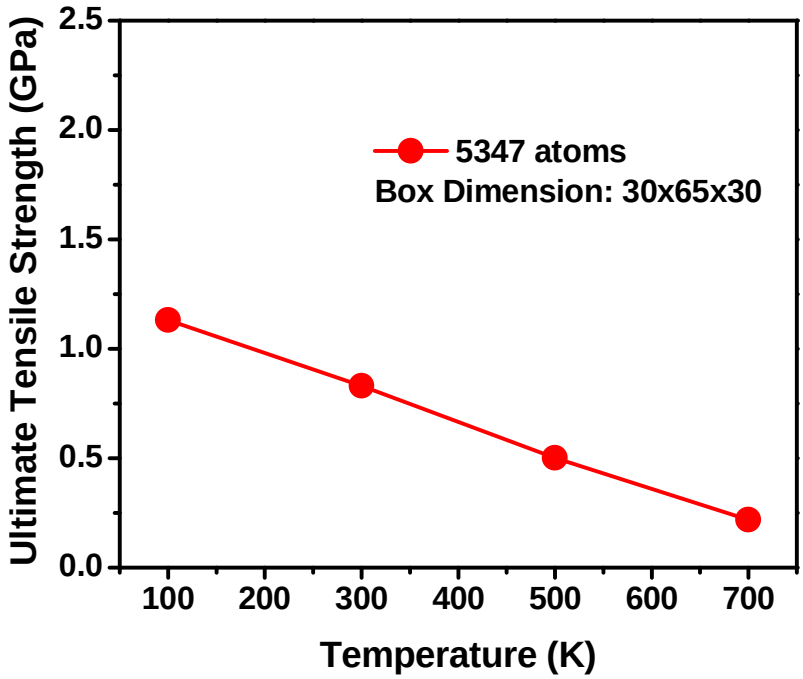

Fig. 4.10: Ultimate Tensile Strength vs. Temperature; Box Dimensions: 30 x 65 x 30

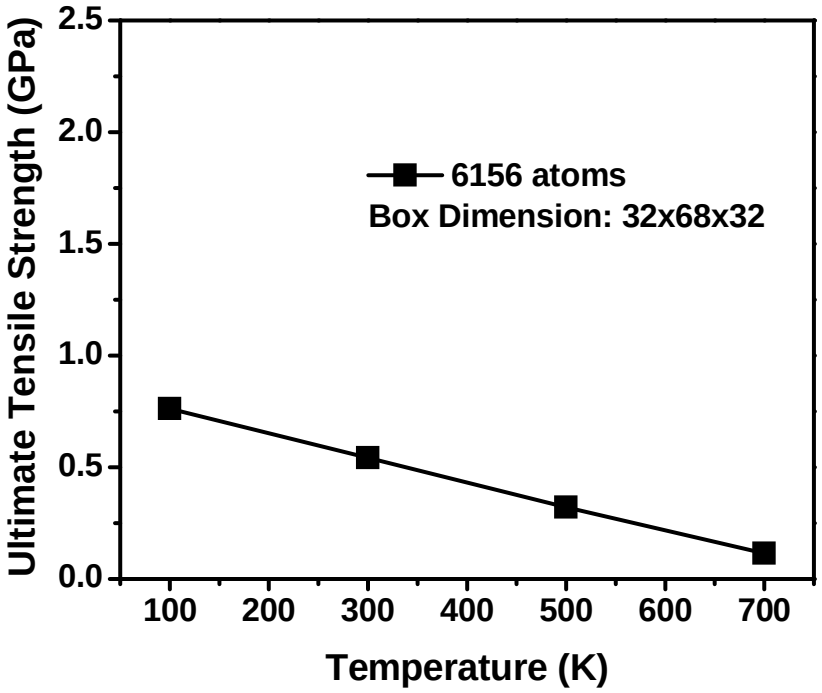

Fig. 4.11: Ultimate Tensile Strength vs. Temperature; Box Dimensions: 32 x 68 x 32

A comparative analysis was done to study the effect of temperature as well as the box dimensions (specimen design) on the ultimate tensile strength of the material in case of Molecular Dynamic simulations. The analysis, showing the variation of UTS with temperature for different box dimensions, is illustrated in Fig. 4.12.

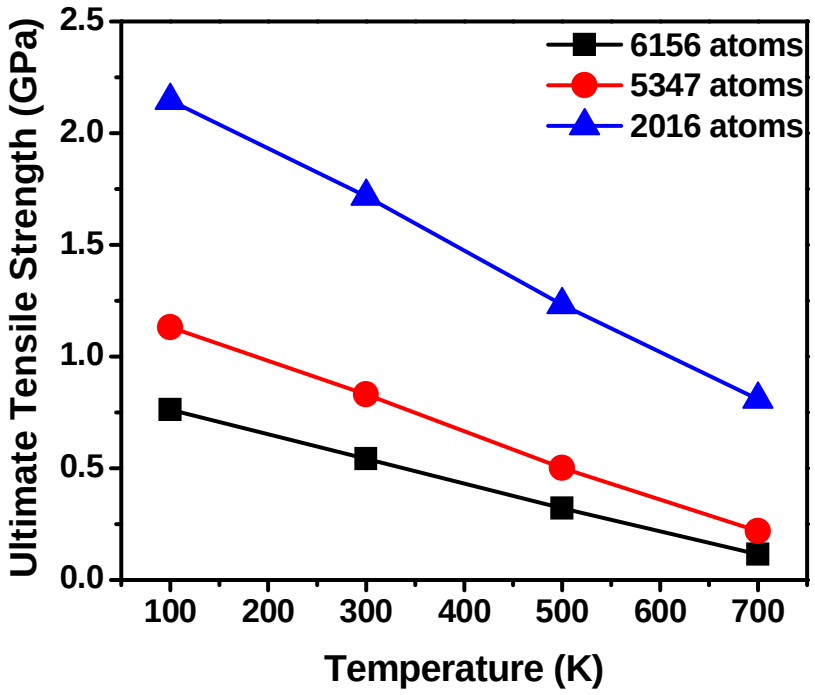

Fig. 4.12: Ultimate tensile strength against temperature for different no. of atoms.

It can be seen that for a particular number of atoms, with the increase in temperature, there is appreciable decrease in the magnitude of UTS.For a sample-box of 2016 atoms, the magnitude of UTSdecreasesup to ≈62 %. On the other hand, the variations in the magnitude of UTS are ≈ 81% and ≈ 85% for sample-boxes consisting of 5347 atoms and 6156 atoms respectively. From theseresults it has been observed that the percentage change in UTS values increases with increase innumber of atoms.

4.2. Uniaxial ratcheting

Ratcheting is a phenomenon, occurring under asymmetric cyclic loading, which refers to accumulation of progressive plastic strain with increase in number of cycles. In case of uniaxial ratcheting, for completion of a cycle, there is an application of load in a specified direction and magnitude of load application on the reverse part is different. There can be several types of loading conditions such as tension-tension, compression- compression and tension -compression loading. Engineering structures usually undergo tension-compression loading during their service life. In our investigation, focus has been given to understand the ratcheting behavior of nanoscale copper for practical purposes.

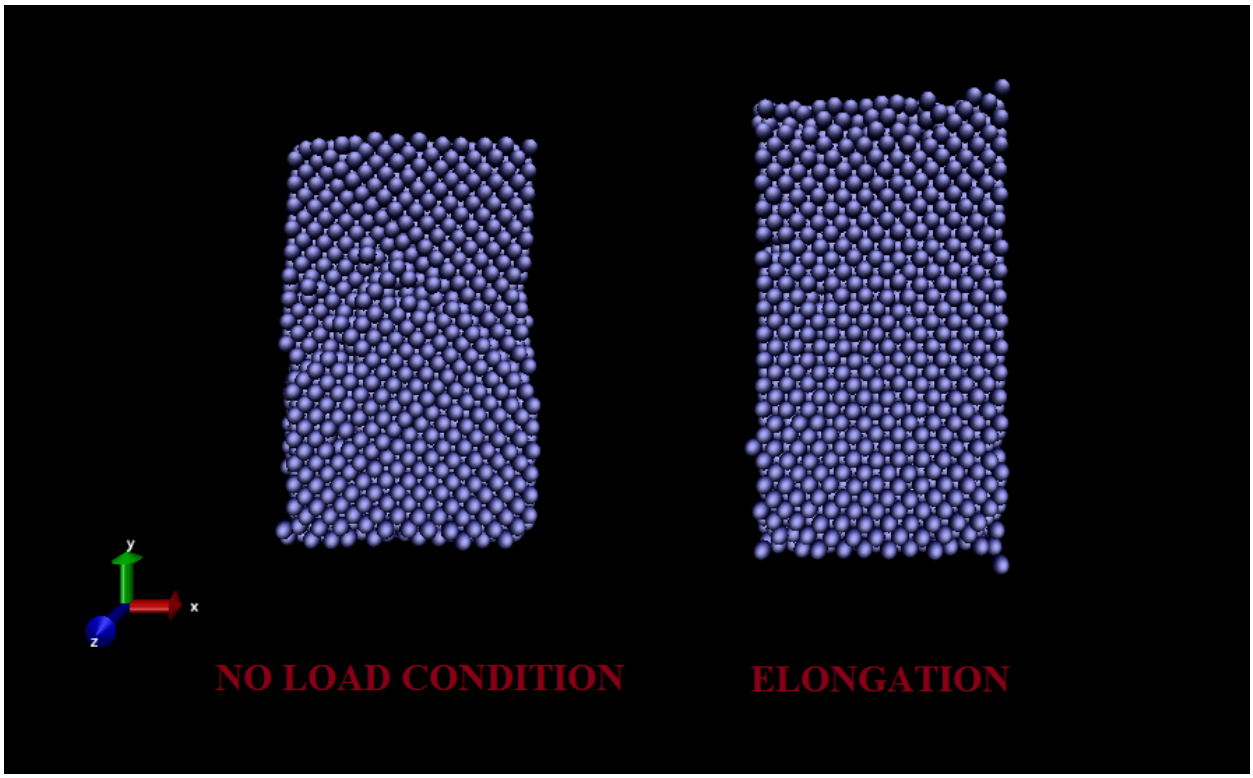

Fig. 4.13: VMD snapshots showing no load condition and elongation at tensile loading of simulation sample during ratcheting.

Hence, VMD snapshots are taken for tension-compression loading during ratcheting. Fig. 4.13 shows comparison of VMD snapshots for the part of the cycle where elongation occurs as a result of tensile loading during ratcheting. VMD snapshot for the other half; when compressive load acts on the simulation box resulting in compression during ratcheting is shown in Fig. 4.14.

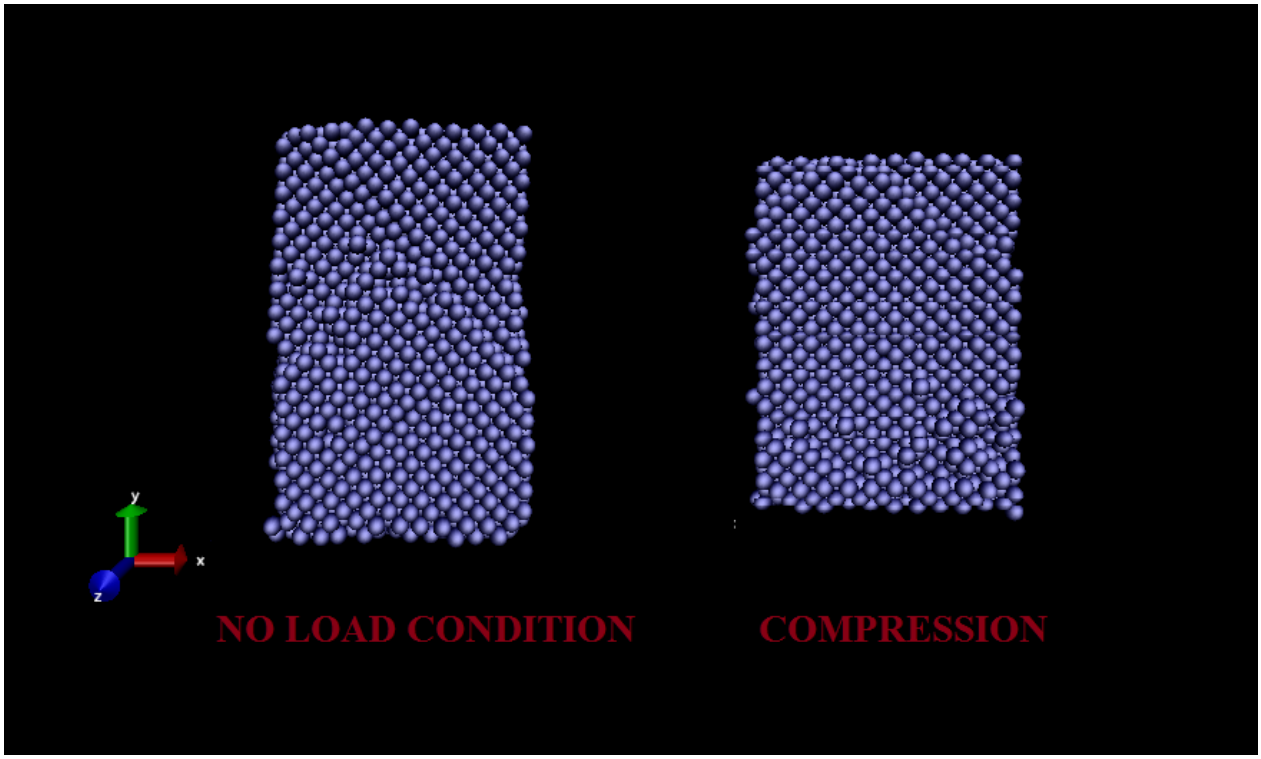

Fig. 4.14: VMD snapshots showing no load condition and compression at compressive loading of simulation sample during ratcheting.

4.2.1 Effect of stress-ratio (R)

Uniaxial ratcheting of nanoscale copper has been conducted by MD simulations as per parameters given in Table 2 (Chapter 3).Variations in accumulation of ratcheting strain with number of cycles for different stress ratios are plotted in Fig. 4.15.

The results illustrated in this plot evidently show that the accumulation of ratcheting strain increases with increase in stress-ratios (R). It can also be observed that there is no appreciable increase in ratcheting strain after a certain number of cycles. Maximum accumulation of ratcheting strain as obtained from these simulations are 4.544%, 4.549% and 4.598% for stress-ratios of R = -0.6, 0.4 and -0.2 respectively.

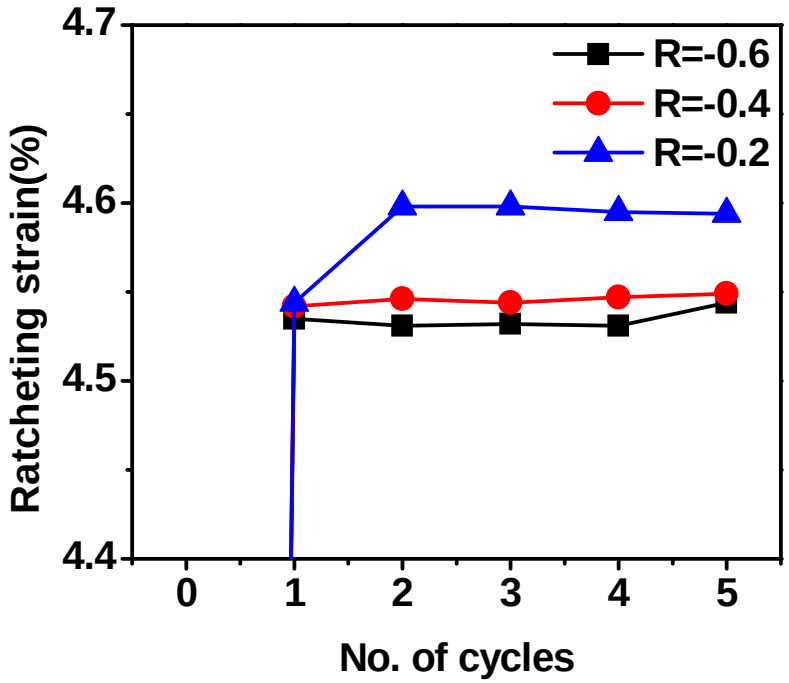

Fig. 4.15: Relationship between ratcheting strain and no. of cycles at various stress ratios at *T* = 300 K.

Experimental observations on ratcheting deformation on metallic materials suggest that strain accumulation gets a saturation level after a certain number of cycles [25, 26]. It can be seen from earlier investigations that saturation cycle for copper alloy is 200 cycles [20], for pure copper is

400 cycles [10].From the simulation results of this investigation, it has been found that accumulation of ratcheting strain nearly becomes constant after two cycles.

4.2.2 Effect of temperature

It is known that materials possess lower strength at high temperature due to softening [25, 26]. If the applied stress is kept constant, greater amount of deformation of a material is expected to occur at higher temperatures as a result of softening. To show the dependence of temperature on ratcheting strain, simulations on uniaxial ratcheting have been conducted in two phases at four different temperatures viz. 100 K, 300 K, 500 K and 700 K.

For the first phase, maximum stress (σ_{max}) is taken as 90% of the UTS value (determined at every temperature) with constant stress ratio (R) of -0.2. Also, the minimum stress (σ_{min}) is calculated for each simulation.Fatigue simulations were then performed and values of ratcheting strain at different temperatures were calculated up to 10 cycles. Subsequently, the variation of ratcheting strain with the number of cycles is studied.

For the second phase, fatigue simulations were carried out at a fixed value of σ_{max} and σ_{min} up to 50 cycles.

These two phases have been stated below:

(a) It is already mentioned in the previous paragraph that σ_{max} for these set of simulations has been taken as 90% of the corresponding UTS values at different temperatures; the calculated σ_{max} values and other parameters used for simulation are as listed in Table3.After 10 cycles of cyclic loading simulations, percentage accumulation of ratcheting strain has been calculated as per equation (3.5), Chapter 3.

A graph showing the variation of ratcheting strain with the number of cycles at different temperatures has been plotted which is shown in Fig. 4.16.

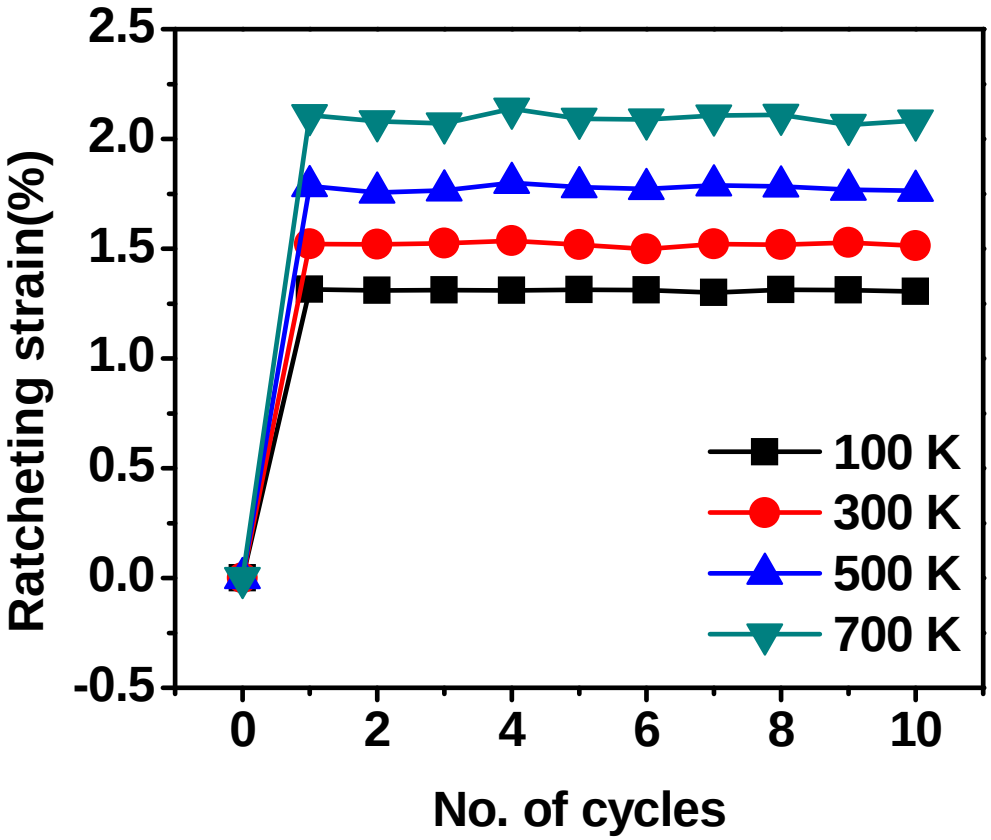

Fig. 4.16: Ratcheting strain vs. no. of cycles at various temperatures at stress ratio (R) = -0.2.

It can be said that with the increase in temperature, there is appreciable increase in ratcheting strain. The average ratcheting strain is observed to be 1.31 %, 1.52 %, 1.8 % and 2.08 % for temperatures 100 K, 300 K, 500 K and 700 K respectively. It can be observed that ratcheting strain at a particular temperature remains nearly constant with increase in number of cycles.

It is known that ratcheting deformation takes place at different rates in different intervals of time [22]. Analogous to creep curves, ratcheting strain vs. number of cycles curve contains three regions; initial sharp increase in strain accumulation, followed by attaining a steady state in the second stage and finally sharp increase in strain up to failure. The phenomenon of attaining a steady state in strain accumulation is commonly termed as stable ratcheting or can be termed as plastic shake down when rate of accumulation of ratcheting strain tends to zero [24].

From the current set of simulation results, the first and second stages could be observed up to 10 cycles. This indicates that the material under investigation achieves a steady state just after the first cycle of loading. This fact needs further verification.

To further verify the authenticity of the first phase, another set of simulations were carried out as given in (b).

(b) To examine the extent of steady state, ratcheting simulations (second phase) have also been carried out up to 50 cycles for a constant value of σ_{max} and σ_{min}. Typical results obtained from these simulations have been illustrated in Fig. 4.17.

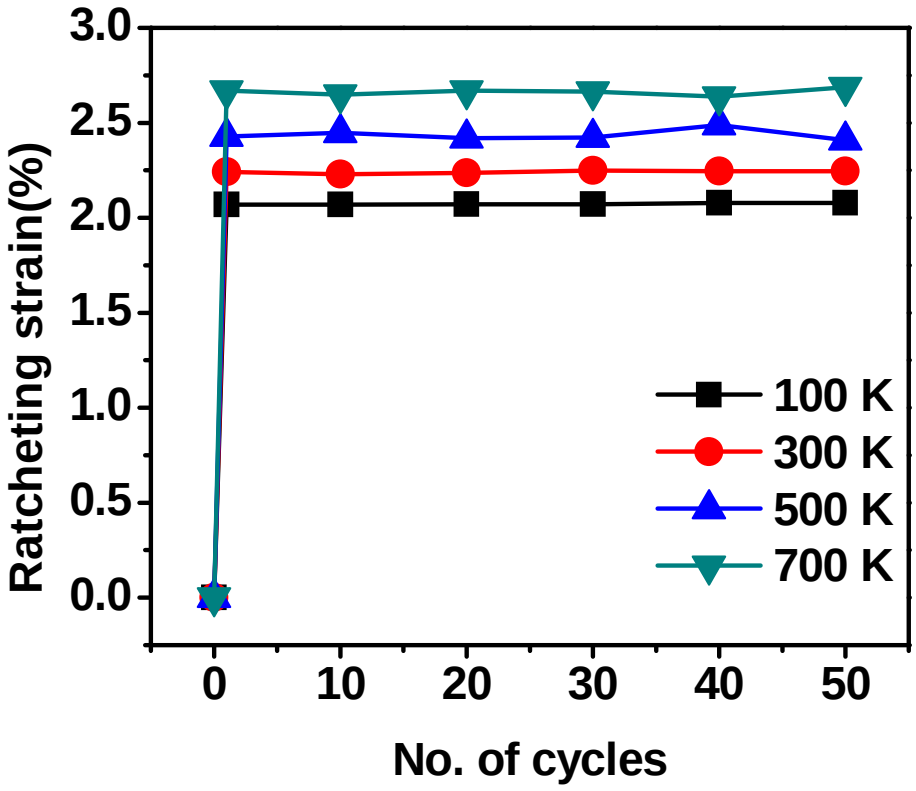

Fig. 4.17: Ratcheting strain against no. of cycles at various temperatures.

It can be seen that there is not much variation in ratcheting strain percentage with increase in number of cycles but it increases with increase in temperature. The average ratcheting strain is observed to be 2.07 %, 2.24 %, 2.44 % and 2.66 % for temperatures 100 K, 300 K, 500 K and 700 K respectively. However, the attainment of third stage could not be seen. It can be expected that simulations up to a larger number of cycles can initiate the third stage.

4.3 Comparative study

Kang et al. [10] have investigated the nature of ratcheting strain accumulation with varying number of cycles with respect to different parameters for different fcc materials. Our investigation deals with nanoscale copper; thus comparison has been done with the results obtained in their experimental works related to pure copper only.

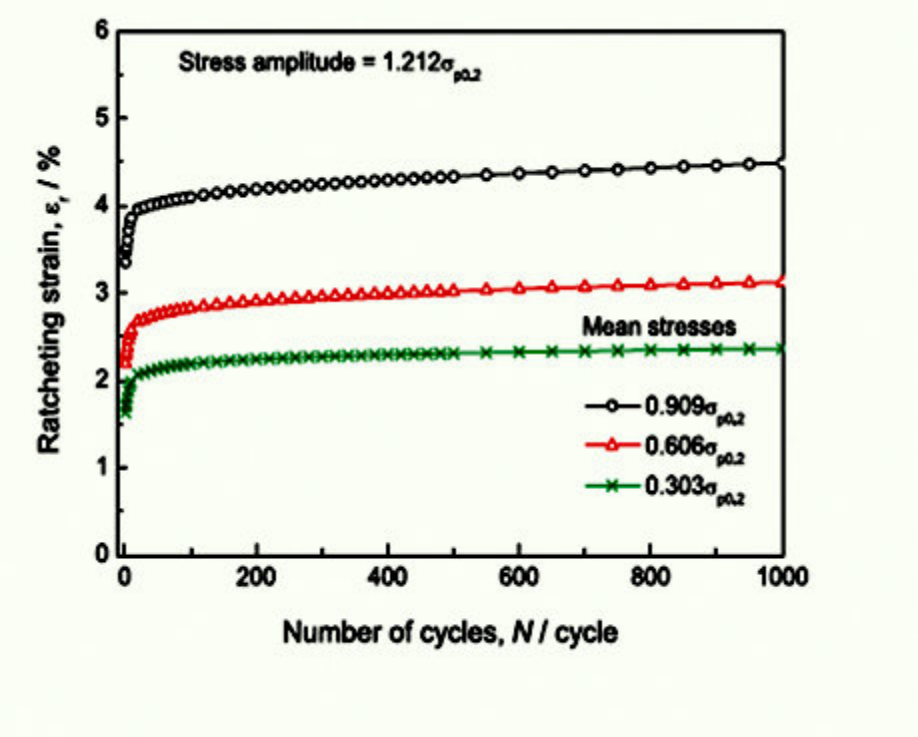

Fig. 4.18: Uniaxial ratcheting results of pure copper at constant stress amplitude and various mean stresses (following [10]).

From their investigation, it can also be stated that ratcheting strain increases with increase in number of cycles. Looking precisely at the curves, the ratcheting strain percent for 5 cycles of cyclic loading is determined. The value of ratcheting strain percent is equal to ≈2.1%, ≈2.6% and ≈3.9% for stress ratios of -0.6, -0.33 and -0.15 respectively. In our investigation as shown in Fig.

4.15, the accumulation of ratcheting strain also decreases with decrease in stress-ratio. The accumulation of ratcheting also increases with the increase in number of cycles of cyclic loading. Thus, the results obtained in our investigation are in accordance with the results found by Kang et al. The value of ratcheting strain percent is equal to ≈4.53%, ≈4.55% and ≈4.61% for stress ratios of -0.6, -0.4 and -0.2 respectively. The ratcheting strain accumulation is found to be greater for MD simulation sample. The difference in ratcheting strain accounts for the use of perfect crystal of copper in MD simulations. This investigation, using molecular dynamics simulation, suggests that MD simulation can well-predict the ratcheting behaviour of copper.

Chapter 5

Conclusions and Future work

OUTLINE

Conclusions

Future Work

5.1. Conclusions:

The influence of temperature and stress ratio on the tensile and ratcheting fatigue behaviour of nanoscale copper have been studied using molecular dynamics simulation. According to simulation results the following conclusions can be derived:

a) The Ultimate Tensile Strength (UTS) of copper is found to decrease with increase in temperature. Subsequent drop in the stress-strain curves at higher temperatures is observed.

b) With variation in sample configuration that is with increase in dimensions of the simulation box, UTS is found to decrease considerably.

c) The results of tensile behaviour indicate that Young's modulus of nanoscale copper shows a decreasing trend with increase in temperature.

d) The results related to ratcheting behaviour of nanoscale copper indicate that with increase in stress ratio (R), accumulation of ratcheting strain increases.

e) For a particular specimen design, the accumulation of ratcheting strain is observed to increase with increase in temperature.

f) A brief comparison of the results from this investigation has been made with those obtained from laboratory experiments. It can be seen that the results obtained through MD simulations is in good agreement with those obtained from laboratory experiments. Thus, it can be suggested that MD simulations can predict ratcheting behaviour of copper.

5.2. Future work:

In this investigation, tensile and ratcheting behaviour of nanoscale pure copper has been studied. Critical analyses of the outcomes of this investigation may lead to the following scopes of further studies:

(i) To study the prolonged effect of temperature on the ratcheting behaviour of nanoscale copper, simulations on ratcheting can be conducted for greater number of cycles (up to 1000 cycles).

(ii) To study the effect of strain rate on tensile behaviour of the materials, simulations on tensile tests can be conducted.

(iii) Similar simulations can be conducted to observe the tensile and ratcheting behaviour of various other fcc materials like nickel, aluminium. The results from these simulations can be used for further analysis and understanding the variation in their ratcheting behaviour.

Chapter 6

REFERENCES

6. REFERENCES:

[1] Z. Xia, D. Kujawski, F. Ellyin, Int. J. Fatigue 18 (1996) 335–341.

[2] R.J. Rider, S.J. Harvey, H.D. Chandler, Int. J. Fatigue 17 (7) (1995) 507–511.

[3] Y. Liu, G. Kang, Q. Gao, A multiaxial stress-based fatigue failure model considering ratchetting–fatigue interaction, International Journal of Fatigue 32(4) (2010) 678-684.

[4] F. Ellyin, Fatigue Damage, Crack Growth and Life Prediction, London, Chapman and Hall Publications (1997).

[5] A. Satyadevi, S.M. Sivakumar, S.S. Bhattacharya, A new failure criterion for materials exhibiting ratcheting during very low cycle fatigue, Materials Science & Engineering A 452-453 (2007) 380-385.

[6] J.W. Ringsberg, Life prediction of rolling contact fatigue crack initiation, International Journal of Fatigue 23 (2001) 575–586.

[7] G. Chen, X. Chen, C-D.Niu, Uniaxial ratcheting behavior of 63Sn37Pb solder with loading histories and stress rates, Materials Science and Engineering A 421 (2006) 238–244.

[8] G. Kang, Uniaxial time-dependent ratchetting of SiC_P/6061Al composites at room and high temperature, Composites Science and Technology 66 (2006) 1418–1430.

[9] C. Gupta, J.K. Chakravarttya, G.R. Reddy, S. Banerjee, Uniaxial cyclic deformation behavior of SA 333 Gr 6 piping steel at room temperature, International Journal of Pressure Vessels and Piping 82 (2005) 459–469.

[10] G. Kang, Y. Liu, Y. Dong, Q. Gao, Uniaxial Ratcheting Behaviours of Metals with Different Crystal Structures or Values of Fault Energy: Macroscopic Experiments, J. Mater. Sci. Technol., 27(5) (2011) 453-459.

[11] X. Feaugas, C. Gaudin, Int. J. Plast. 20 (2004) 643–662.

[12] C. Gaudin, X. Feaugas, Acta Mater. 52 (2004) 3097–3110.

[13] G.Z. Kang, Q. Gao, X.J. Yang, Int. J. Mech. Sci. 44 (8) (2002) 1645–1661.

[14] L.J. Chen, Z.G. Wang, G. Yao, J.F. Tian, Int. J. Fatigue 21 (1999) 791.

[15] H. Inoue, Y. Akahoshi, S. Harada, Mater. Sci. Res. Int. 1 (1995) 95– 99.

[16] B. Li, L. Ries, M.de Freitas, Simulation of cyclic stress/strain evolutions for multiaxial fatigue life prediction, International Journal of Fatigue 28 (2006) 451–458.

[17] W.J. Chang, Molecular-dynamics study of mechanical properties of nanoscale copper with vacancies under static and cyclic loading, Microelectronic Engineering 65 (2003) 239–246.

[18] W.J. Chang, T.H. Fang, Influence of temperature on tensile and fatigue behavior of nanoscale copper using molecular dynamics simulation, Journal of Physics and Chemistry of Solids 64 (2003) 1279–1283.

[19] http://lammps.sandia.gov - Sandia National Laboratories, (2012).

[20] C.-B. Lim, K.S. Kim, J.B. Seong, Ratcheting and fatigue behavior of a copper alloy under uniaxial cyclic loading with mean stress, International Journal of Fatigue 31 (2009) 501–507.

[21] P. Murali, T. Guo, Y. Zhang, R. Narasimhan, Y. Li, H. Gao, Atomic scale fluctuations govern brittle fracture and cavitation behaviour in metallic glasses, Phys. Rev. Lett. 107 (2011) 215-501.

[22] G. Z. Kang, Y.G. Li, J. Zhang, Y.F. Sun, Q. Gao, Theor. Appl. Fract. Mech. 43 (2005) 199–209.

[23] M.I. Mendelev, M.J. Kramer, C.A. Becker, M. Asta, Analysis of semi-empirical interatomic potentials appropriate for simulation of crystalline and liquid Al and Cu, Phil. Mag. 88 (2008) 1723-1750.

[24] X. Yang, Int. J. Fatigue 27 (2005) 1124–1132.

[25] G. E. Dieter, Mechanical Metallurgy, London, Mc-Graw Hill Publication (1988).

[26] R.W. Hertzberg, Deformation and fracture mechanics of engineering materials, New York, John Wiley & Sons, Inc. (1989).